MODELING OF STRESS DEVELOPMENT IN AEROGEL PREPARATION

by

BETÜL ÜNLÜSÜ

B.S. in Ch.E., Boğaziçi University, 1996

Submitted to the Institute for Graduate Studies
Science and Engineering in partial fulfillment of
the requirements for the degree of
Master of Science
in
Chemical Engineering

Boğaziçi University
1998

ACKNOWLEDGEMENTS

I would like to express my deepest appreciation to Assoc. Prof. Sermin Gönenç SUNOL for her supervision and support during my study. I would also like to thank to Prof. Dr. Amable HORTAÇSU and Prof. Dr. Aydın SUNOL for their interest in commenting on my thesis.

Graduate assistantship granted throughout my study by the Department of Chemical Engineering and financial support donated by Boğaziçi University Research Fund (Project No:96A0520) are acknowledged.

I would like to thank to my friends Zerrin Bağcı, Neşe Kurt, Leyla Özkan, Mehmet Bozan, Ali Cem Erginsoy, Burak Alakent, Taner Zafer Şen, Göktuğ Ahunbay, Banu Yaşar, Deniz Ardal and Mete Altıntaş for everything we shared.

I'm grateful to my family for their encouraging love.

Finally, I would like to dedicate this thesis to those free-minded and honest people who made and will make contributions in science and engineering.

ABSTRACT

Aerogels are prepared by sol-gel method associated with supercritical drying. They are used in different areas due to their special characteristics such as high porosity, low density, low thermal conductivity. Drying is one of the critical steps in producing aerogels with desired properties, since drying stresses can cause shrinkage and cracking during the process.

In this study, stress development during heating to the critical temperature of pore liquid is modeled for an elastic, isotropic, circular plate. The flow of pore liquid in the radial direction is neglected and Darcy's Law is applied for the flux in the axial direction. The model, which is an integro-differential equation, derived for a free circular plate is analyzed where radial constraint is in effect. Radial constraint prevents the pore liquid from escaping the network in the radial direction. Also, the expansion of the network in this direction is prevented. When radial constraint is applied, the difference between a circular plate and a cylinder of high thickness disappears since the flow is in the axial direction and the most significant stress occurs in the radial direction in both cases.

The model equations are solved to observe the effects of heating rates, shear moduli and permeability of the network. The presence of syneresis, spontaneous shrinkage due to condensation reactions, is also examined.

The magnitudes of stresses determined at different conditions for the cylindrical silica gel are compared to the modulus of rupture which is 0.2 MPa for the alcogel and 2 MPa for the aerogel. The aim is to determine whether or not production of crack-free monolithic materials is possible under specified conditions. It is observed that, radial constraint increases stress development significantly and fracture of the cylinder is inevitable. Therefore, heating rate is decreased to a very low value (0.04 °C/min). Actually, increasing temperature 0.04 °C per minute doesn't have a physical meaning since with that rate, it takes about four days to reach the critical temperature. Even at this low heating rate, the magnitude reaches about 0.4 MPa at low temperatures and it even exceeds 2MPa when syneresis is taken into account.

The analysis is repeated for a circular plate. The effect of heating rate, shear modulus and permeability are studied. It is observed that stress formation is lower in comparison to the cylindrical silica gel. Since the modulus of rupture of the circular plate is not known, a comparison with the magnitudes of the computed stresses could not be made.

The model can be applied to any porous material and used to find the optimum heating rates for aerogel production .

ÖZET

Aerojeller, kritik-ötesi kurutma işlemi ile birleştirilmiş sol-jel yöntemi ile üretilirler. Bu maddeler, yüksek gözeneklilik, düşük yoğunluk, yüksek ısıl iletkenlik gibi özellikleri nedeniyle değişik alanlarda kullanılabilirler. Kurutma, bu sırada oluşan gerilimler yapıda büzülme ve kırılmaya neden olabileceğinden, istenen özelliklere sahip aerojel üretimindeki en önemli aşamalardandır.

Bu çalışmada, gözenek sıvısının kritik sıcaklığına kadar ısıtma sırasındaki gerilim oluşumu, elastik ve eşyönsel olan dairesel bir plaka için modellenmiştir. Gözenek sıvısının çap yönündeki akışı ihmal edilmiş ve z yönündeki akış için Darcy Kanunu benimsenmiştir. Serbest dairesel plaka için çıkarılmış, integro-diferansiyel bir denklem olan model, çap yönünde konulmuş kısıt için incelenmiştir. Bu durumda, gözenek sıvısı çap yönünde akamaz ve jel yapısı bu yönde genleşemez. Çap yönünde kısıt uygulandığında, dairesel plaka ile yüksek kalınlıktaki bir silindir arasındaki fark kaybolur. Çünkü, her iki durumda da akış z yönündedir ve en yüksek gerilimler çap yönünde oluşur.

Model denklemleri, ısıtma hızının, esneklik katsayısı ve jel yapısının geçirgenliğinin etkisini incelemek üzere çözülmüştür. Jel yapısının yoğunlaşma tepkimeleri sonucu büzülmesi de dikkate alınmıştır.

Geometrisi silindir olan silika jeli için değişik koşullarda hesaplanmış gerilimler, alkojel için 0.2 MPa ve aerojel için 2 MPa olan kırılma katsayısı ile karşılaştırılmıştır. Amaç, belirli koşullar altında, tek parça halinde malzeme üretme olanağının olup olmadığını belirlemektir. Yapılan hesaplar sonucunda, çap yönündeki kısıtın, gerilim oluşumunu önemli ölçüde artırdığı ve silindirin kırılmasının kaçınılmaz olduğu görülmüştür. Bu nedenle ısıtma hızı çok düşük bir değere indirilmiştir (0.04 °C/dk.). Aslında, sıcaklığı dakikada 0.04 °C artırmanın fiziksel bir anlamı yoktur. Çünkü bu ısıtma hızıyla kritik sıcaklığa ulaşmak yaklaşık dört gün sürmektedir. Bu çok düşük ısıtma hızında bile oluşan gerilimin büyüklüğü, düşük sıcaklıklarda 0.4 MPa ulaşmakta ve yoğunlaşma tepkimelerinden kaynaklanan büzülme hesaba katıldığında 2 MPa değerini geçmektedir.

Aynı hesaplar, dairesel plaka için de yapılmıştır. Isıtma hızının, esneklik katsayısının ve geçirgenliğin etkisi incelenmiştir. Dairesel plakada gerilim oluşumunun silindirden daha düşük olduğu görülmüştür. Dairesel plakanın, kırılma katsayısı bilinmediği için, hesaplanmış gerilimlerle bir karşılaştırma yapılamamıştır.

Model, gözenekli maddelere uygulanabilir ve aerojel üretiminde en iyi ısıtma hızlarını bulmakta kullanılabilir.

TABLE OF CONTENTS

LIST OF FIGURES

Page

Page

LIST OF TABLES

LIST OF SYMBOLS

A	Cross Sectional Area
D	Permeability
E	Young's Modulus
F_L	Force applied on the liquid
F_S	Force applied on the solid
G	Shear Modulus
J	Liquid Flux
K	Bulk Modulus
P	Stress in the liquid
P_C	Capillary Pressure
P_L	Pressure in the liquid
r_C	Capillary Radius
T	Temperature
t	Time
V_L	Volume of liquid
α_L	Thermal expansion coefficient of liquid
α_S	Thermal expansion coefficient of solid
ε	Volumetric strain
$\dot{\varepsilon}$	Volumetric strain rate
ε_f	Free strain
ε_s	Syneresis strain
ϕ	Porosity
γ_{LV}	Liquid-vapor interfacial energy
ν	Poisson ratio
η_L	Viscosity of the liquid
ρ	Solid fraction of the network
σ	Total stress
$\tilde{\sigma}$	Stress on the solid

1. INTRODUCTION

Aerogels are inorganic oxides such as silica, alumina that are produced by sol-gel process followed by supercritical drying technique. The unique properties of aerogels allow them to be used in very different areas. They are used as catalysts or catalyst substrates since they have high porosity (Pajonk, 1991). Aerogels are materials of very low thermal conductivity. Therefore, they are employed in window insulation. Another characteristics of aerogels is their low refractive indices. This allows them to be used as particle detectors in high energy physics experiments. Also, aerogel monoliths are utilized to produce glass and glass ceramics (Ayen and Iacobucci, 1988).

Sol-gel process includes the hydrolysis and condensation of alkoxide precursors. In the process, the first step is the preparation of a colloidal form, sol, of a metal oxide. Then, a gel, a continuous solid matrix immersed in a continuous liquid phase, forms because of the condensation of partially hydrolyzed species into a three dimensional network (Ward and Ko, 1995). The gel must be dried to remove the liquid in the pores. There are three techniques for the removal of the pore liquid: Evaporation, supercritical drying and freeze drying.

Evaporation of the pore liquid is usually carried at near ambient temperatures possibly under vacuum or by heating up the system to higher temperatures. The products of this process are called xerogels. Xerogels are low porosity-high density materials, in comparison to the aerogels that are produced by supercritical drying technique, since during evaporation, their pores collapse. The pore collapse could be best explained through interfacial phenomena. During the pore evacuation process, vapor-liquid interface forms and this causes formation of capillary stress. The gel network shrinks because of these large stresses (Brinker and Scherer, 1990).

Freeze-Drying, which involves freezing of the pore liquid and subliming the resulting solid under vacuum, is one way of preventing the formation of liquid-vapor interface. The product is called a cryogel. In this method, pressure gradient forms because of draining the

pore liquid toward crystalline layer at the surface. Also, growing crystals can stretch and tear the network (Scherer, 1993).

Supercritical drying techniques provide processing routes for evacuation without forming vapor liquid interface. Several methods are developed to remove the pore liquid at supercritical conditions. In the first method, heating up the system filled with liquid rises the temperature and pressure above critical constants. Then the system is depressurized. (Schmitt et al., 1993). Another way is pressurizing the system with an inert gas such as nitrogen or argon, then heating the system to exceed critical temperature of the liquid (Mulder and Van Lierop, 1986). Solvent exchange method can also be used. The pore liquid is replaced by liquid carbon dioxide, then the system is brought to supercritical conditions (Rangarajan and Lira, 1991). The forth method is the supercritical carbon dioxide extraction in a semi continuous system (Ayen and Iacobucci, 1988). In the last method, the system is pressurized with carbon dioxide, then the mixture of pore liquid and carbon dioxide is brought to supercritical conditions (Sunol et al., 1994), (Sunol et al., 1995), (Sunol et al., 1996).

Supercritical drying technique eliminates capillary forces by providing a one phase system but there are other causes for stress formation. During heating to reach the supercritical conditions, the solid matrix can not expand at a comparable rate with the one of liquid. Therefore, the liquid stretches the network while the network applies a compressive stress on the liquid (Scherer, 1992). Cracking of the network can occur during diffusion step if the diffusion time is not long enough (Novak and Knez, 1997). Also, stresses can form at depressurization step. If the depressurization rate is too high, the fluid inside the gel can not flow from the gel-network at a comparable rate. The pressure out of the gel will decrease faster than the pressure inside. Therefore, the gel will swell and cracking occurs (Scherer, 1994a), (Scherer, 1994b).

Modeling of the supercritical drying step to compute stress formation is useful to determine optimum heating rates, diffusion times and depressurization rates. It is necessary to know deformation and flow characteristics of the gel network to model the system. Theory of deformation relates the shrinkage of the network to the stress in the liquid and fluid is

transported either by diffusion or by flow down a pressure gradient (Brinker and Scherer, 1990).

In this study, stress development during heating step of supercritical drying is modeled for a geometry of circular plate. It is assumed that the plate shows elastic behavior and it is isotropic which means that the elastic properties such as Young's modulus, Poisson ratio are the same in every direction. Also, the presence of radial constraint is considered and the model equation derived is solved to examine the effects of heating rates, shear moduli and permeability of the network on stress formation.

Chapter 2 of the thesis is literature survey that covers general information, theory of deformation and drying methods for porous materials and modeling of supercritical drying sections. Model equations are derived and solution methods are presented in Chapter 3. Results and discussion are given in Chapter 4. Conclusions and recommendations are enclosed in Chapter 5. The user-defined subroutines of PDECOL package written in Fortran code and the program made via PDEase2D are presented in Appendices A and B respectively.

2. LITERATURE REVIEW

This review encloses the synthesis of porous materials by sol-gel technique, deformation and flow theories in gels, drying methods to produce xerogels, aerogels, and cryogels and models developed for supercritical drying.

2.1. General Concepts on Aerogels and Related Porous Materials

Aerogels are inorganic oxides such as silica, alumina, that are produced by sol-gel method followed by supercritical drying. They are porous solids which have large surface areas, extremely low thermal conductivities and high chemical activity.

Aerogels are prepared from gels which can be produced from metal alcoxides. The first step in the preparation of gels is the formation of a colloidal material, or sol. If the liquid phase is water, it is an aquasol, if it is alcohol, the sol is an alcosol. Gels are formed from sols. Gels are also colloidal systems. They include a continuous solid phase and a continuous liquid phase. If the liquid in the pores of the gel is water, the gel is an aquagel, if alcohol, it is an alcogel.

Drying an alcogel requires the removal of the pore liquid and its replacement with a dry gas. The process used to remove the pore liquid affects the characteristics of the dried gel. Therefore, gels are also classified according to the drying method. If the liquid in the gel is removed by evaporation, the gel is called xerogel. If the gel is dried by supercritical drying technique it is an aerogel as explained and if the pore liquid first frozen into a solid and then sublimed, the resulting gel is called cryogel (Gesser and Goswami, 1989).

2.2. Sol-Gel Method

Sol-gel method is the formation of a sol followed by a formation of a gel. A sol is a colloidal suspension of solid particles in a liquid and a gel is one molecule which has macroscopic dimensions so that it extends throughout the solution. A gel has a continuous solid skeleton and a continuous liquid phase enclosed by the solid. Gels are formed from particulate sols, when attractive dispersion forces make them to stick together to form a network

Sol-gel chemistry can be described in terms of two classes of reactions with an alkoxide ($M(OR)_n$) as a precursor:

Hydrolysis $\quad -MOR + H_2O \rightarrow -MOH + ROH$

Condensation $\quad -MOH + ROM- \rightarrow -MOM- + ROH$

or

$\quad -MOH + HOM- \rightarrow -MOM- + H_2O$

This description of the sol-gel process expresses two points. First, a gel forms because of the condensation of partially hydrolyzed species into a three-dimensional gel network. Second, the properties of the gel are determined by the factors affecting these reactions. These factors are called sol-gel parameters such as type of precursor, type of solvent, water content, acid or base content, precursor concentration and temperature.

The gel must be dried to remove the solvent. Aging time which is between the formation of the gel and drying is also an important parameter because the gel is dynamic during this step and it continues to undergo hydrolysis and condensation reactions. In addition, syneresis, which is spontaneous shrinkage of the gel network due to bond formation or attraction between particles, occurs during drying (Ward and Ko, 1995).

2.3. Deformation and Flow in Gels

Theory of deformation and flow in gels deals with the flow of liquid in the pores and the deformation of solid skeleton of a gel during syneresis and drying. Theory of deformation relates the pressure in the liquid to shrinkage of the network. Liquid transport includes the processes of fluid flow.

If a body is suspended from a polymeric filament, the strain will increase slowly. When the stress is removed, the strain starts to disappear. This behavior is called creep and it is the result of the viscoelasticity of polymeric substances. In case of an elastic material, initial dimensions recover immediately while a viscous material never returns to its initial dimensions after the removal of stress (McCrum et al., 1994).

If a stress σ_x is applied to a viscoelastic material, the total strain along the x axis:

$$\varepsilon_x = \varepsilon_E + \varepsilon_D + \varepsilon_V \tag{2.1}$$

which is also equal to:

$$\varepsilon_x = \frac{\sigma_x}{E} + \frac{\sigma_x}{E_D}\varphi(t) + \frac{\sigma_x t}{3\eta} \tag{2.2}$$

The first term on the right hand side is instantaneous elastic strain (ε_E), the second is the delayed elastic strain (ε_D), and the last term is the viscous strain (ε_V). Stress in the x direction is denoted by σ_x, and η is viscosity. E is the Young's modulus. The creep function φ, is dependent on time and it can have values between 0 and 1. Viscoelastic and viscous behavior under constant stress are described in Figure 2.1. When the stress is removed, the recovery of the instantaneous elastic strain is immediate. On the other hand, the delayed strain disappears gradually. The viscous or plastic strain never recovers (Brinker and Scherer, 1990).

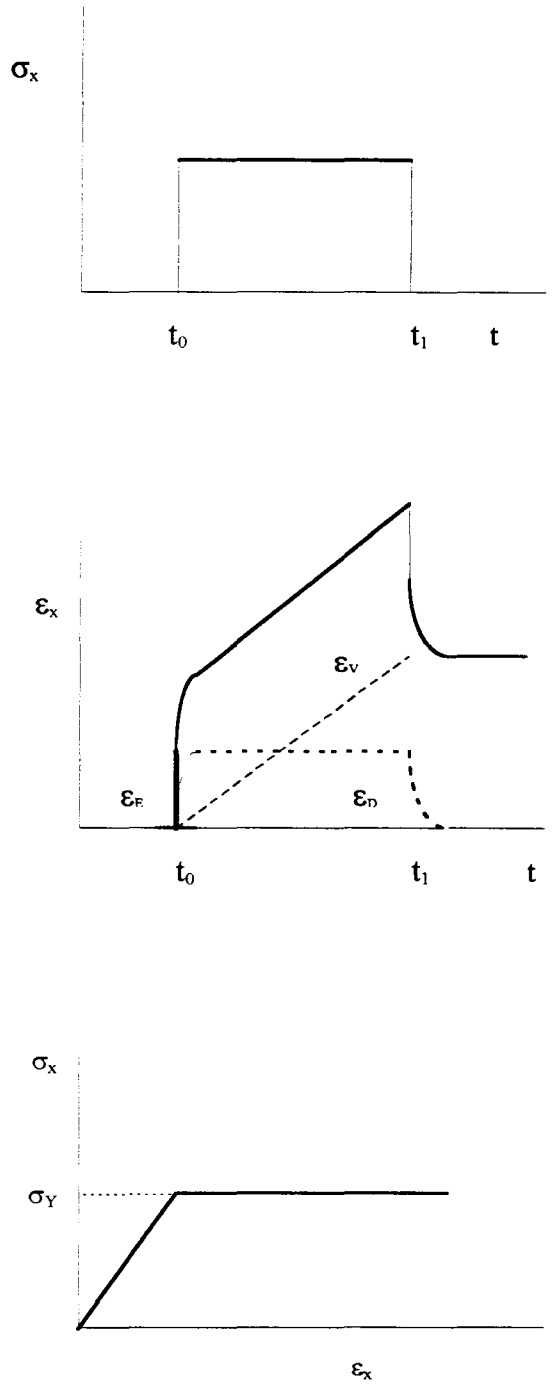

Figure 2.1. Schematic illustration of strain when viscoelastic and viscous materials are subjected to a constant stress.

When a tensile force is applied to the end of an elastic bar, it gives an instantaneous elastic response. Its length increases and its width decreases. The ratio between the strain in the

direction of the applied force and the one in the perpendicular direction is called Poisson Ratio (Timoshenko and Goodier, 1970).

$$\frac{\varepsilon_y}{\varepsilon_x} = -\nu \tag{2.3}$$

If uniformly distributed forces are applied on an elastic material, the following equations govern the system

$$\varepsilon_z = \frac{1}{E}\left(\sigma_z - \nu\left(\sigma_y + \sigma_x\right)\right) \tag{2.4}$$

$$\varepsilon_y = \frac{1}{E}\left(\sigma_y - \nu\left(\sigma_z + \sigma_x\right)\right) \tag{2.5}$$

$$\varepsilon_x = \frac{1}{E}\left(\sigma_x - \nu\left(\sigma_y + \sigma_z\right)\right) \tag{2.6}$$

Here E is the modulus of elasticity or Young's modulus. If strains in all the directions are added, volumetric strain ε is found in terms of the total stress σ and theYoung modulus E (Brinker and Scherer, 1990).

$$\varepsilon = \frac{1}{E}\left[(1-2\nu)\right]\sigma \tag{2.7}$$

$$\varepsilon = \frac{\sigma}{3K} \tag{2.8}$$

where K is the bulk modulus and it is defined as

$$K = \frac{E}{3(1-2\nu)} \tag{2.9}$$

These equations are adapted to porous structures and for a porous cube of porosity 1-ρ (Figure 2.2.), the constitutive equations, the relationship between the stresses formed and strains that result, are developed.

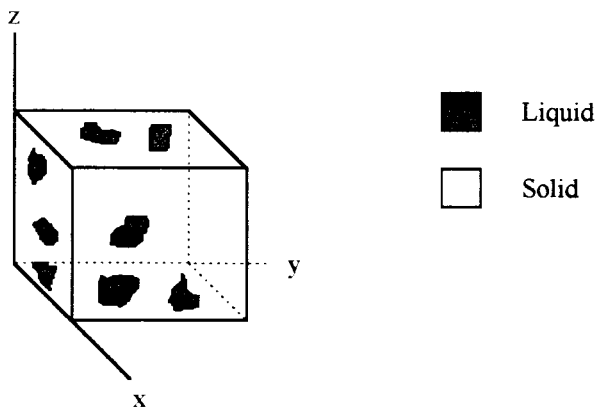

Figure 2.2. Schematic illustration of a cube of gel.

The shaded parts in Figure 2.2, show the intersection of liquid with the faces of the cube. If forces F_x, F_y and F_z are applied to the surfaces of the cubic gel; the forces on the liquid and solid phases can be expressed in terms of volume fraction of the solid.

$$F_{xL} = F_x(1-\rho) \tag{2.10}$$

$$F_{xS} = F_x\rho \tag{2.11}$$

The total surface area A of the cube is shared by the liquid A_L, and solid phases A_S.

$$A_L = A(1-\rho) \tag{2.12}$$

$$A_S = A\rho \tag{2.13}$$

The stress on the solid phase is:

$$\tilde{\sigma}_x = \frac{F_x \rho}{A \rho} = \frac{F_x}{A} \tag{2.14}$$

For the stress-strain relationship, the presence of the liquid phase must be taken into the account. The pressure in the liquid phase is

$$P_L = -\frac{F_{xL}}{A_L} \tag{2.15}$$

The negative sign in P_L implies that the pressure in the liquid is tensile. The stress in the liquid, P, is the same expression without the negative sign since stress is positive when it is tensile according to the sign convention.

$$P = \frac{F_{xL}}{A_L} \tag{2.16}$$

The total stress on the cube face is

$$\sigma_x = \frac{F_{xS} + F_{xL}}{A} \tag{2.17}$$

When the expressions for forces on the liquid and solid phases are inserted, the following equation is found for the total stress.

$$\sigma_x = \tilde{\sigma}_x + (1-\rho)P \tag{2.18}$$

Liquid applies hydrostatic stress which affects each component of strain equally. Therefore, in the presence of liquid and solid phases, stress-strain relationships are as follows:

$$\varepsilon_z = \frac{1}{E}\left(\tilde{\sigma}_z - \nu\left(\tilde{\sigma}_y + \tilde{\sigma}_x\right)\right) + cP \tag{2.19}$$

$$\varepsilon_z = \frac{1}{E}\left(\tilde{\sigma}_z - \nu\left(\tilde{\sigma}_y + \tilde{\sigma}_x\right)\right) + cP \tag{2.20}$$

$$\varepsilon_z = \frac{1}{E}\left(\tilde{\sigma}_z - \nu\left(\tilde{\sigma}_y + \tilde{\sigma}_x\right)\right) + cP \tag{2.21}$$

where c is a constant that must be determined (Brinker and Scherer, 1990).

2.4. Drying

Sol-gel method must be followed by a drying process in order to remove the liquid from the alcogel. This process influences porous structure and mechanical properties of the gel. The change in the characteristics are affected by the drying conditions. Three different ways of drying are evaporation, freeze drying and supercritical drying.

2.4.1. Evaporation

In this method, porous liquid is allowed to evaporate either at ambient temperature and pressure or heat is given to the system. Evaporation can be divided into several stages.

2.4.1.1. Constant Rate Period: In this period, pores are totally filled with liquid and evaporated liquid is replaced by diffusion easily (Figure 2.3.). If heat is not given to the system, the difference between the pressures at the bottom (at the surface) and at the top of the boundary layer does not change and the rate of evaporation remains constant (Brinker and Scherer, 1990).

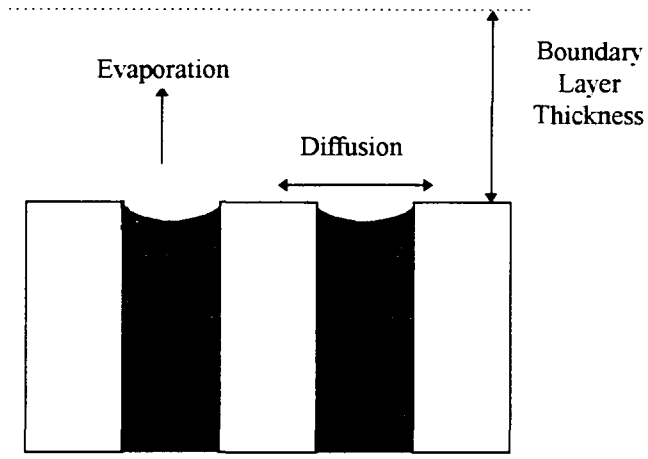

Figure 2.3. Illustration of boundary layer formed during evaporation.

The capillary pressure depends on capillary radius r_c and the energy associated with the liquid vapor interface γ_{LV} by Laplace's equation.

$$P_c = \frac{2\gamma_{LV}\text{Cos}\theta}{r_c} \tag{2.22}$$

Suction in the liquid phase (negative pressure) creates compressive stresses on the solid and this causes shrinkage of the structure. Shrinkage, which is equal to the volume of the liquid evaporated, continues until the gel becomes so rigid that the vapor-liquid menisci penetrate into the gel. Therefore the extent of shrinkage at constant rate period depends on the capillary pressure exerted by the pore liquid and the bulk modulus of the solid. The compressive stresses in terms of capillary pressure and volume fraction of porosity ϕ are defined as follows:

$$\tilde{\sigma} = \tilde{\sigma}_x + \tilde{\sigma}_y + \tilde{\sigma}_z = 3\phi P_C \tag{2.23}$$

2.4.1.2. Critical Point of Drying: The network becomes more stiff as the evaporation proceeds. When the modulus of the solid balances the capillary pressure, shrinkage stops. This is the critical point at which the vapor-liquid menisci penetrate into the structure and unsaturated pores appear (Brinker and Scherer, 1990).

2.4.1.3. First Falling Rate Period: In this stage, menisci penetration into the body causes the formation of a liquid film (Figure 2.4). The liquid flows along the film to reach the surface because evaporation continues mostly at the exterior surface. Liquid evaporates in the pores and vapor diffuses to the surface at a minor level, because of the decrease in temperature and vapor pressure between the interior to the exterior part of the body.

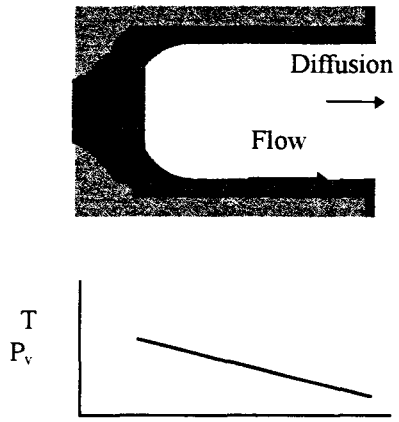

Figure 2.4. Liquid-vapor meniscus retreated in the body and temperature and vapor pressure along its thickness.

The driving force for flow of the liquid is the gradient in the capillary pressure. The rate of liquid flow is governed by Darcy's Law (Brinker and Scherer, 1990).

2.4.1.4. Second Falling Rate Period: At the previous stage, evaporation at the surface continues since the evaporated liquid is replaced by the flow from the interior of the body. As the menisci recede more in the pores, the driving force for the liquid flow decreases. At the second falling rate period, flow stops and liquid is removed just by the evaporation in the pores (Brinker and Scherer, 1990).

2.4.2. Freeze Drying

The presence of liquid-vapor interface and capillary pressure can be avoided by freezing the pore liquid and subliming the resulting solid under vacuum. This process is called freeze drying and it is widely used in food processing. Because the growing crystals reject the gel network, and pushing it out of the way until it is stretched to the breaking point, this method is not suitable to produce monolithic aerogels. On the other hand, gels are used as hosts of crystals for the same reason. The gel is so effectively excluded that the crystals nucleated in the pore liquid are not contaminated with the gel phase; the crystals can grow up to a size of a few millimeters before the strain is so large that macroscopic fractures appear in the gel. The product obtained by freeze drying method is called cryogel. If a silica gel is frozen, flakes of silica gel are produced; if freezing is done unidirectionally, fibers of gel are obtained (Scherer, 1993).

There are several reasons for deformation during freeze drying. First, draining of liquid toward crystalline layer at the surface can create pressure gradient in the pores, leading to differential shrinkage and fracture. Second, crystals growing from internal nuclei can stretch and tear the network material. Third, freezing of bulk liquid can produce blade-like dendrites that can cut through the gel.

In principle, if the network is strong enough to withstand the stress exerted by the crystals, then a gel could be freeze-dried without shrinkage and damage. Such a cryogel would have an open structure and low density similar to an aerogel.

2.4.3. Supercritical Drying

Removing the pore liquid by evaporation causes shrinkage and cracking, caused by capillary forces. One way of avoiding liquid-vapor interface and capillary forces is drying the gel network at supercritical conditions. When critical temperature T_c and critical pressure P_c of the liquid are exceeded, the formation of two phases are prevented and the product aerogel has more preferable characteristics such as high surface area, porosity, chemical activity and resistance to heat treatment. Such material is first produced by Kistler in 1932 (in Pajonk, 1991). Alcogels, rather than hydrogels are produced due to lower critical properties of alcohol (Table 2.1).

Five methods have been developed up to now to dry alcogels at supercritical conditions. In the first method, solvent is brought to supercritical conditions by heating up the system to increase temperature and pressure (Schmitt et al., 1993). In the second method, the system is pressurized by an inert gas prior to heating (Mulder and Van Lierop, 1986). The third method, the solvent is substituted with liquid carbon dioxide which is vented out of the system at supercritical conditions (Rangarajan and Lira, 1991). This method is preferred due to T_c and P_c of carbon dioxide (Table 2.1). The fourth method suggests supercritical carbon dioxide extraction in a semi continuous system for the removal of alcohol) (Ayen and Iacobucci, 1988). In the fifth method, the system is pressurized with carbon dioxide and carbon dioxide-alcohol mixture is brought to supercritical conditions to vent off the supercritical fluid (Sunol et al., 1994), (Sunol et al., 1995), (Sunol et al., 1996).

Table 2.1. Critical temperatures and pressures of selected solvents

Substance	**Formula**	**T_c (°C)**	**P_c (MPa)**
Carbon dioxide	CO_2	31.1	7.36
Ethanol	CH_3OH	240	7.93
Methanol	C_2H_5OH	243	6.36
Water	H_2O	374	22.0

2.4.3.1. Autoclave Drying: In this method, silica alcogel is placed into an autoclave. The autoclave is filled with ethanol prior to pressurization so that the pressure increases to values above the critical pressure of the ethanol when the system is heated. While the temperature is increased to 275 °C, a pressure of approximately 120 bar is reached (Schmitt et al., 1993). In Figure 2.6., pressure temperature path followed during the process is shown. The disadvantage of the process is the evaporation of liquid out of the pore during heating where capillary action in pores may be effective.

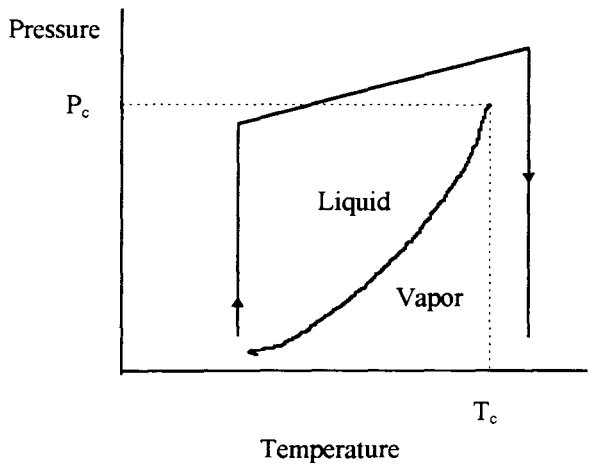

Figure 2.5. Temperature- pressure path followed during the supercritical drying process

2.4.3.2. Supercritical Drying with Pressurization by an Inert Gas: In this method, boiling of the pore liquid is suppressed by first pressurizing the system by an inert gas nitrogen or argon.

In a work by Mulder and Van Lierop (Mulder and Van Lierop, 1986), SiO_2 aerogels are prepared with Nitrogen pressurization. The pore liquid which must be removed is ethanol. The steps of the process are as follows: First prepressurization of nitrogen is applied up to 80 bar. Then system is heated with a rate of 50 °C/h until 300 °C is reached. The pressure increases due to the expansion of nitrogen as well as to the evaporation of ethanol (Figure 2.5). For the decompression step, rate depends on the size of the sample. For gels prepared

in 15mm diameter tubes, the rate is 150 bar/h while the gels of 80 mm diameter, decompression is 15 bar/h. After this step, the system is cooled down.

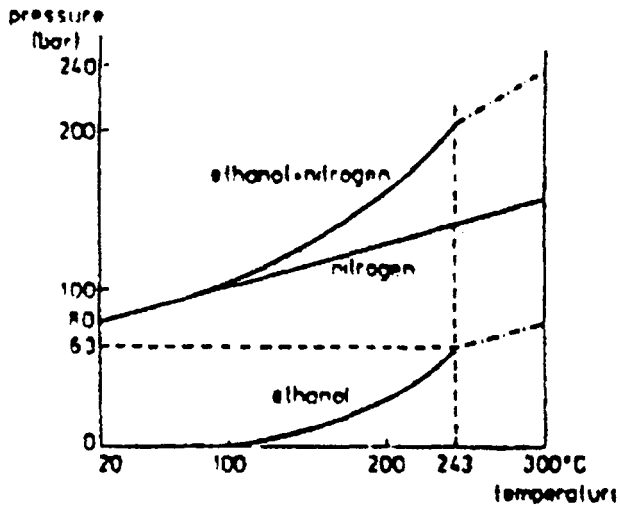

Figure 2.6. Pressure increase with heating, after pressurization with N_2 (Mulder and Van Lierop, 1986).

The application of the inert gas pressure in the autoclave improves the properties of gel prepared by supercritical drying since the amount of the inert gas applied affects the shrinkage of the gels. It is claimed that, aerogels of no shrinkage can be produced with a pressure of 80 bar (Table 2.2).

Table 2.2. Effect of Nitrogen Pressure on Density and Percent Shrinkage.

N_2 pressure (bar)	**specific density (g/cm^3)**	**shrinkage (%)**
0	0.49	73 (cracked)
10	0.27	52
40	0.14	7
80	0.13	0

2.4.3.3. Supercritical Carbon Dioxide Extraction: In this method, the alcogel is placed into the extractor. Carbon dioxide at 235 bar is passed through the extraction vessel that is kept at 40 °C.

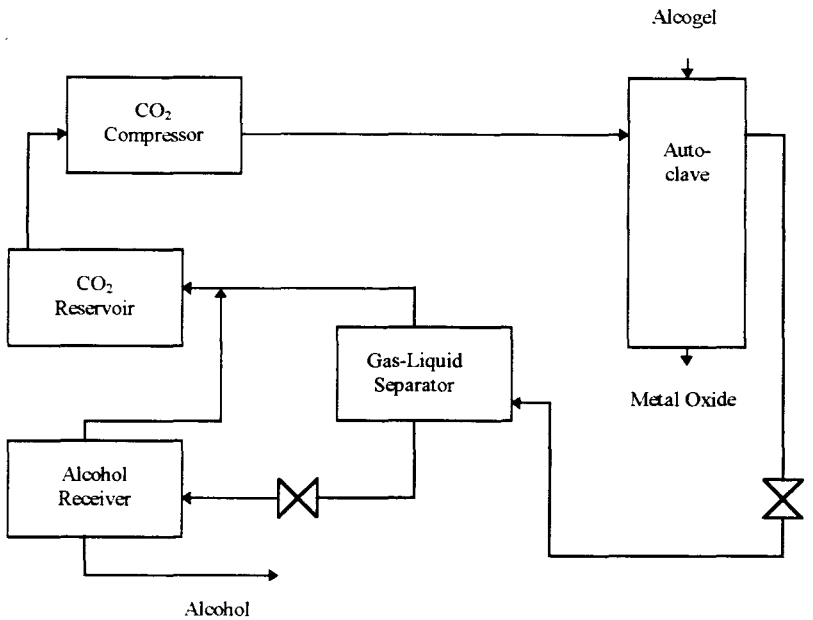

Figure 2.7. Supercritical fluid extraction process

Supercritical carbon dioxide extracts the alcohol. The pressure of the outlet stream, which consists of carbon dioxide and alcohol, is reduced across the metering valve in order to have a liquid alcohol and gaseous carbon dioxide and then the mixture is separated. Recovered carbon dioxide is recycled (Figure 2.7). The extraction is continued until no alcohol is detected in the separator. The autoclave is then depressurized and the aerogel is removed from the vessel (Ayen and Iacobucci, 1988).

2.4.3.4. Solvent Exchange Method: In this method, the liquid in the pores is displaced by ethanol that is miscible with both water and carbon dioxide. This is done because the miscibility of water with carbon dioxide is very low Thus, applying carbon dioxide to the system before displacement with ethanol causes formation of two phases and results in interfacial tension. Therefore, the gel is put into a high pressure autoclave filled with

ethanol. Ethanol extracts the water in pores. The time for this step depends on the size of the sample. Then, liquid carbon dioxide at about 16-20 °C is pumped to the system until a pressure of 100 bar is reached. Liquid carbon dioxide diffuses into the gel and extracts ethanol. After sufficient time for solvent exchange, the temperature of the system is increased to 40 °C and supercritical carbon dioxide is vented out of the system (Rangarajan and Lira, 1991).

2.4.3.5. Supercritical Drying with Carbon Dioxide Pressurization: In this method, the system is pressurized to 80 atmospheres with carbon dioxide. Carbon dioxide feed is compressed before it is fed to the vessel that contains the alcogel. After the predetermined pressure is reached, the sandbath heater housing the drying vessel is heated so that a temperature above the critical value of carbon dioxide-alcohol mixture is reached (Figure 2.8). The heating rates used are 1°C/min (low heating rate), 10 °C/min (high heating rate) and flash heating. The system is kept under these conditions for a specified time. Then the supercritical fluid is vented out of the system keeping the temperature of the reactor constant. At the end of the experiment, the gel is swept with fresh carbon dioxide to remove remaining trace amounts of alcohol and water. Then the system is cooled and the aerogel is removed (Sunol et al., 1994), (Sunol et al., 1995), (Sunol et al., 1996).

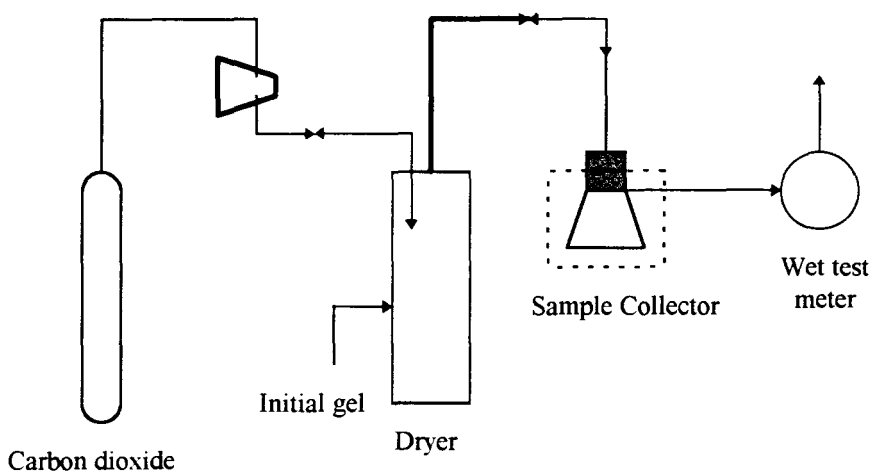

Figure 2.8. Experimental set-up for supercritical drying with carbon dioxide pressurization

2.5. Modeling of Supercritical Drying

Modeling of drying phenomena is essential in understanding the stresses formed and controlling the degree of shrinkage. The ability to predict shrinkage during drying would assist in production of advanced materials for thermal insulation (here, the target is negligible shrinkage), optical films (where shrinkage is desired for the control of porosity/refractive index). Drying phenomena is also important in areas such as production of microporous adsorbents and membranes where large shrinkage is desirable to have smaller pores. In addition, drying conditions are the determining factor for gel cracking.

Supercritical drying eliminates capillary stresses which form during evaporation but shrinkage and cracking can still occur for some reasons. Differential strain between the pore liquid and gel network during heating, acceleration of syneresis at high temperatures, short diffusion times and high depressurization rates are some of the reasons. Also, there can be some operational errors. The pore liquid can boil by not including enough liquid in the autoclave. The impurities in the liquid can raise critical point.

The models derived for heating, diffusion and depressurization steps of supercritical drying are described in the following sections.

2.5.1. Stress Development in Supercritical Drying during Heating Step

In a study by Scherer (Scherer, 1992), a model is derived to determine stress development during heating of the alcogel. The geometry of the material dried is cylindrical. Liquid flux is only in the radial direction. The basis of the effort is expressing volumetric strain in two different ways. First, the volume of the liquid that flows out of a slice of network must be equal to the volumetric contraction of that part. Therefore, an expression for the rate of total volumetric strain rate ($\dot{\varepsilon}$), in terms of liquid flux J, volumetric solid fraction ρ,

heating rate $\dot{T}$, expansion coefficients of both solid α_S, and liquid phases α_L, is derived (Scherer, 1991).

$$\dot{\varepsilon} = 3(1-\rho)\alpha_L \dot{T} + 3\alpha_S \dot{T} - \nabla \cdot J \tag{2.24}$$

Second, it is derived starting from the total hydrostatic stress on the network and strains caused by syneresis $\dot{\varepsilon}_s$, heating and strain caused by the stress in the pore liquid, P.

$$\dot{\varepsilon} = 3\dot{\varepsilon}_s + 3\alpha_S \dot{T} - \frac{\partial}{\partial t}\left[\frac{\beta P + (1-\beta)\langle P\rangle}{K}\right] \tag{2.25}$$

where

$$\beta = \frac{1+\nu}{3(1-\nu)} \tag{2.26}$$

with ν is the Poisson ratio for the network.

The average stress in the pore liquid is given by

$$\langle P\rangle = \frac{2}{R^2}\int_0^R P(r)\, r\, dr \tag{2.27}$$

The dimensionless differential equation obtained from the two equations for the volumetric strain is as follows:

$$\frac{1}{u}\frac{\partial}{\partial u}\left(u\frac{\partial y}{\partial u}\right) = \frac{\partial y}{\partial \theta} + f(\theta) \tag{2.28}$$

The dimensionless variable introduced is u=r/R

and

$$f(\theta) = 3(\dot{\varepsilon}_T - \dot{\varepsilon}_s)\tau + \left(\frac{1-\beta}{\beta}\right)\frac{\partial\langle y\rangle}{\partial\theta} \tag{2.29}$$

with

$$\dot{\varepsilon}_T = (1-\rho)(\alpha_L - \alpha_s)\dot{T} \tag{2.30}$$

$$y = \frac{\beta P}{K} \tag{2.31}$$

$$\langle y\rangle = 2\int_0^1 y(u,\theta)\, u\, du \tag{2.32}$$

The reduced time θ, is defined by

$$\theta = \int_0^t \frac{dt'}{\tau(t')} \tag{2.33}$$

where τ, the relaxation time, is

$$\tau = \frac{\beta\eta_L R^2}{DK} \tag{2.34}$$

Here η_L, R and D stand for the viscosity of the pore liquid, radius of the cylinder and permeability of the network respectively.

The equations are manipulated by making use of Bessel and Laplace Transforms and then solved numerically (Scherer, 1992). After determining the stress formed in the pore liquid, the axial stress in the cylindrical gel is determined from the equation (Scherer, 1992):

$$\sigma_z = \frac{E}{1-\nu}(\varepsilon_z - \varepsilon_f) = \left(\frac{1-2\nu}{1-\nu}\right)(P - \langle P \rangle) \tag{2.35}$$

Change in axial stress with temperature as determined from Equation 2.35 is presented in Figure 2.10. for different values of shear modulus G.

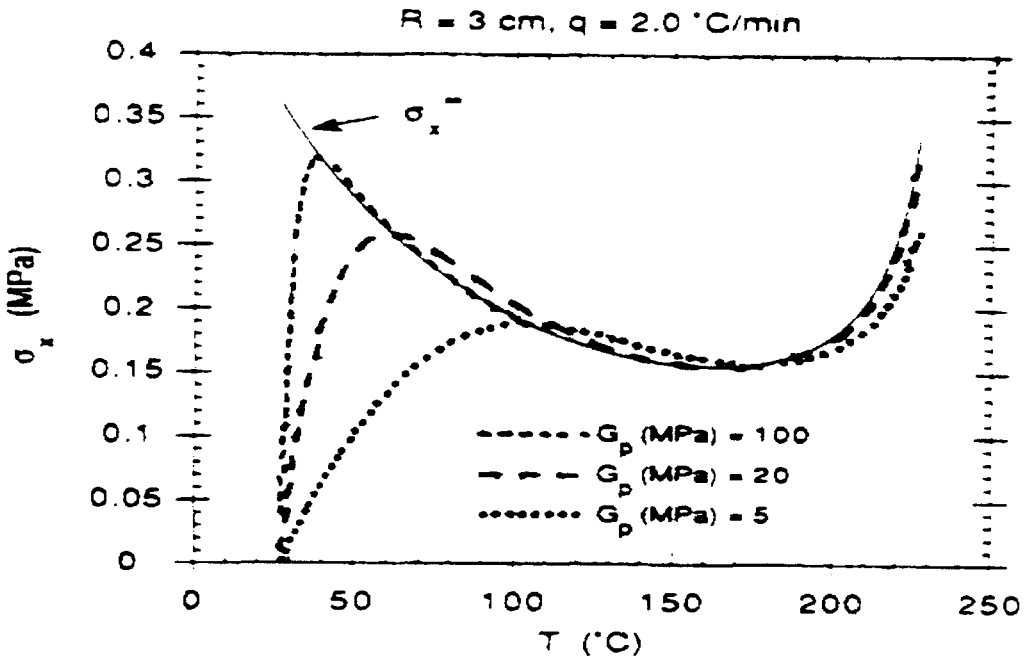

Figure 2.9. Stresses calculated from Equation 2.34 (Scherer, 1992).

The modulus of rupture for alcogel and aerogel are measured and it is determined whether the gel would crack.

2.5.2. Stress Development in Supercritical Drying during Diffusion Step

If alcohol extraction with liquid or supercritical carbon dioxide is used, diffusion of alcohol through the alcogel to carbon dioxide is important and the quality and shapes of aerogel

samples also depend on the diffusion times. If the diffusion time is short, the gel will crack. If the diffusion time is long enough, transparent, crack-free gels can be produced. In a study by Novak (Novak and Knez, 1997), diffusion coefficients of methanol in both liquid and supercritical carbon dioxide are determined from the dependence of the width of the damaged area on diffusion times. A finite cylinder is taken as the intersection of an infinite cylinder of radius r_0 with an infinite cylinder of thickness δ_z. The concentration of methanol can be expressed as follows:

$$C(F_0, R, Z) = f_r\left(F_0, \frac{r}{r_0}\right) f_z\left(F_0, \frac{z}{\delta_z}\right) \tag{2.36}$$

here r/r_0=R and z/δ_z = Z are dimensionless coordinates and f_1 and f_2 are the solutions for the infinite cylinder and infinite plate respectively. F_0, Fourier number for the cylinder, is defined as

$$F_0 = \frac{D_{AB}t}{r_0^2} \tag{2.37}$$

where D_{AB} is diffusion coefficient of methanol-carbon dioxide, t is the diffusion time. If $r_0 < \delta_z$, the concentration of five percent is as follows:

$$C_{5\%} = f_r\left(F_0, R_{5\%}\right) f_z\left(F_0, r_0\right) \tag{2.38}$$

Then the dimensionless width of the damaged area inside the gel sample, R is determined as

$$R_{5\%} = g\left(F_0, C_{5\%}, r_0\right) \tag{2.39}$$

The explicit solution of the equation is the product of logarithmic, cosine and Bessel functions. The quality of the aerogel samples obtained at different diffusion times and temperatures can be observed in Figure 2.10. The quality varies from totally damaged to perfect transparent monoliths. The kinetic parameter D_{AB} can be found by the comparison

of the theoretical model with experiments to predict the drying time for the production of crack-free monoliths.

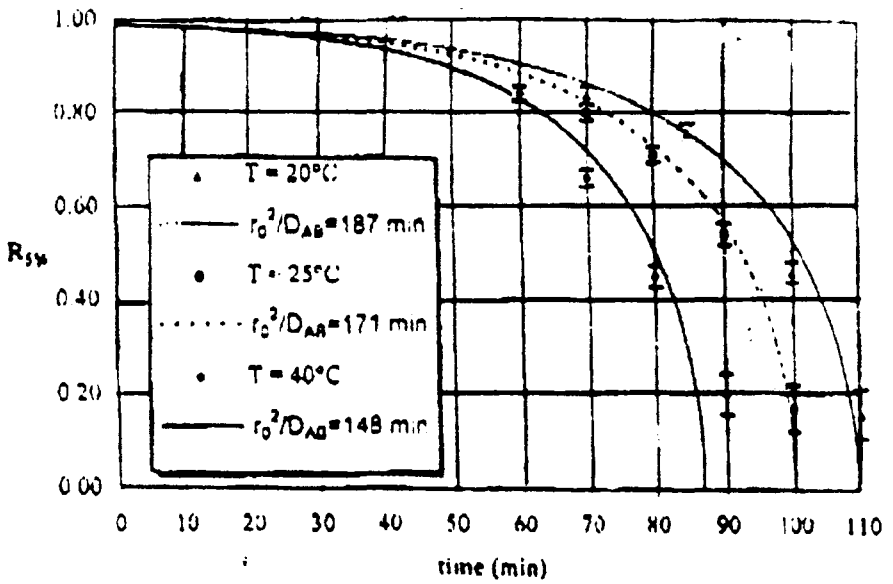

Figure 2.10. Change in damaged area with time (Novak and Knez, 1997).

2.5.3. Stress Development in Supercritical Drying during Depressurization Step

Cracking can occur during depressurization, if the supercritical fluid is released too rapidly from the vessel. During depressurization step, as the vapor is vented from the autoclave, the vapor inside the gel expands and flows out of the reactor. If the depressurization rate is too fast, the vapor can not find time to flow out of the gel and makes it swell like a balloon and crack.

In a study by Scherer (Scherer, 1994a), an analysis is done for the magnitude of stresses formed during depressurization of the autoclave. The transport of the compressible fluid in the pores and the mechanical properties of the network are taken into consideration. For a

cylindrical, spherical, or planar gel (with the appropriate definition of average pressure in the liquid $\langle P_F \rangle$), a continuity equation is derived.

$$(1-\rho)\left(\frac{\rho_f}{\rho_F}\right)+\frac{\partial}{\partial t}\left[\frac{\beta P_F+(1-\beta)\langle P_F\rangle P_A}{K}\right]=\frac{1}{\rho_F}\nabla\cdot\left(\frac{\rho_F}{\eta_F}\nabla\cdot P_F\right) \qquad (2.40)$$

The equation is solved numerically (Scherer, 1994b). Also an approximate analytical solution is derived for the time and spatial distribution of P_F and this is utilized to determine stress development during depressurization.

The stress is found to increase with the size of the sample and the rate of depressurization and it is larger in a cylinder than in a sphere, because the expanding vapor escapes more readily from the sphere. The calculated stresses are large enough so that cracking of aerogels is inevitable (Scherer, 1994b).

3. THEORY

The theory consists of three sections. In the first section, the model equation is derived. In the second one, the solution methods are explained. In the third one, properties of the silica gel-network that are used in solving the model equation are presented.

3.1. Modeling of Heating Step in Supercritical Drying

A constitutive model describing the relationship between the stresses formed and the strains that result during the heating step to reach supercritical conditions, is developed for a circular plate.

3.1.1. The Geometry of the Gel Network

The geometry chosen is a circular plate whose thickness is lower than its radius.

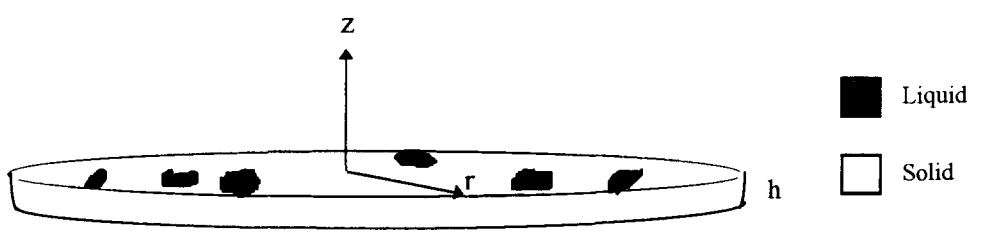

Figure 3.1. Illustration of a circular porous plate

Plates are classified into three categories according to their thickness; thick plates, thin plates (or plates of medium thickness), and very thin or flexible plates (also called plates

with large deflections). A thick plate is the one whose thickness is more than 1/5 of its smaller dimension. A plate is sometimes considered thin when its thickness to the smallest dimension ratio is less than 1/5 but generally the ratio of 1/10 is desired. For lower values, flexible plates are in question. In that case, the classification is also dependent on deflections (Nowinsky, 1978).

3.1.2. Assumptions

Several simplifying assumptions related to the geometry, to liquid flow and material properties are made in the derivation of the model.

For a plate, the flux in the radial direction is neglected, and the flux in the z direction is taken into account since the thickness/radius ratio is low. For the flow of the pore liquid, Darcy's Law, which states that the flux of liquid is proportional to the pressure gradient in the liquid,. is applied and diffusion is neglected. Elastic behavior is assumed for the gel network. Also, the system is taken as isotropic. Therefore, the elastic properties are the same in every direction.

3.1.3. Derivation of the Constitutive Equation

If a slice of gel of area A and thickness Δz is considered, the volume of liquid (V_L) that flows out of the slice must be equal to the volume change or volumetric contraction of the slice.

Taking a slice of infinitesimal thickness Δz in the plate (Figure 3.2).

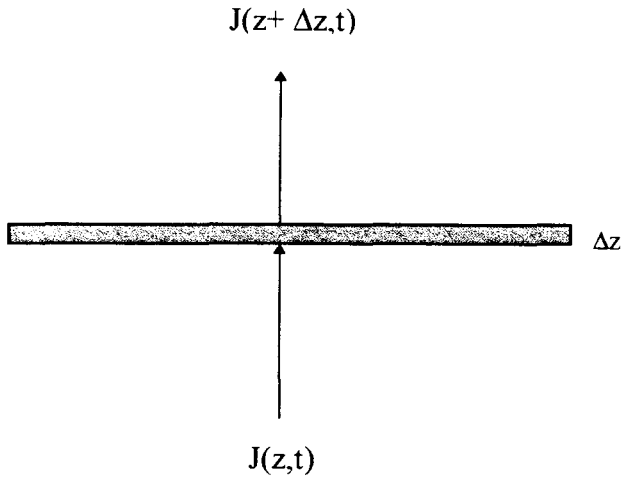

Figure 3.2. A slice of gel of area A and thickness Δz

The volume of liquid in the slice is,

$$V_L = A\Delta z(1-\rho) \tag{3.1}$$

where the volumetric solid fraction ρ is defined as:

$$\rho = \frac{V_S}{V_S + V_L} \tag{3.2}$$

Thermal expansion of liquid due to heating is:

$$\alpha_L = \frac{1}{3V}\frac{dV}{dT} \tag{3.3}$$

Material balance for the volume of fluid in the slice is:

in - out + generation = accumulation

$$\underbrace{AJ(z,t)\Delta t}_{\text{in}} - \underbrace{AJ(z+\Delta z,t)\Delta t}_{\text{out}} + \underbrace{V_L(z,t)3\alpha_L \Delta T}_{\substack{\text{volumetric} \\ \text{thermal expansion}}} = \underbrace{V_L(z,t+\Delta t) - V_L(z,t)}_{\text{accumulation}} \quad (3.4)$$

Dividing both sides by $V_L(z,t)\ \Delta t$ and taking limit as Δz and $\Delta t \rightarrow 0$

$$-\frac{1}{1-\rho}\frac{\partial J}{\partial z} + 3\alpha_L \frac{dT}{dt} = \frac{\dot{V}_L}{V_L} \quad (3.5)$$

Here, $\dot{V}_L$ represents the partial derivative of fluid volume with respect to time.

Fluid flux J is defined according to Darcy's Law as:

$$J = \frac{D}{\eta_L}\nabla P \quad (3.6)$$

Change in liquid volume relates to the volumetric strain rate $\dot{\varepsilon}$ because fluid flow into any region of the gel is equal to local dilatation of the network.

$$\dot{\varepsilon} = \frac{\dot{V}_L + \dot{V}_S}{V_L + V_S} \quad (3.7)$$

Solid network also dilates because of thermal expansion of the solid.

$$\dot{V}_S = 3\alpha_S V_S \dot{T} \quad (3.8)$$

Substituting $\dot{V}_S$ from Equation 3.8 and ρ from Equation 3.2 into Equation 3.7

$$\dot{\varepsilon} = (1-\rho)\frac{\dot{V}_L}{V_L} + 3\alpha_S \rho \dot{T} \quad (3.9)$$

From Equations 3.5 and 3.9

$$\dot{\varepsilon} = 3(1-\rho)\alpha_L \dot{T} + 3\alpha_S \rho \dot{T} - \frac{\partial J}{\partial z} \tag{3.10}$$

Flux is given according to Darcy's Law

$$\frac{\partial J}{\partial z} = \frac{\partial}{\partial z}\left(\frac{D}{\eta_L}\frac{\partial P}{\partial z}\right) \tag{3.11}$$

Stress varies only in the z direction. At the lower surface, there is no flow while liquid can flow freely at the upper surface, therefore, stress in the liquid is zero there.

The free strain of the network is,

$$\varepsilon_f = \varepsilon_s + \alpha_s \Delta T + c'P \tag{3.12}$$

Free strain rate can be explained as the linear contraction rate of the network when the forces are locally in balance. which means if there is tension in the liquid, there is also compression on the network. On the other hand, stress varies from point to point in the gel network Therefore, each region is subjected to an additional stress caused by neighboring regions which makes the local strain rate differs from free strain rate.

The volumetric strain is,

$$\varepsilon = 3\varepsilon_f + \left(\frac{1-2\nu}{E}\right)\sigma \tag{3.13}$$

Here σ denotes the total stress whose derivation is shown in the section 3.1.4.

Substituting the expression found for total stress into Equation 3.13 gives:

$$\varepsilon = 3\varepsilon_f + \left(\frac{1-2\nu}{E}\right)\left[\frac{2E\left(\varepsilon_r - \varepsilon_f\right)}{1-\nu}\right] \tag{3.14}$$

or

$$\varepsilon = 3\varepsilon_f + 2\left(\frac{1-2\nu}{1-\nu}\right)\left(\varepsilon_r - \varepsilon_f\right) \tag{3.15}$$

After rearranging Equation 3.15, the volumetric strain is found as:

$$\varepsilon = \frac{1+\nu}{1-\nu}\varepsilon_f + 2\left(\frac{1-2\nu}{1-\nu}\right)\varepsilon_r \tag{3.16}$$

ε_r is derived in section 3.1.4.

$$\varepsilon_r = \frac{1}{2h}\int_{-h}^{h}\varepsilon_f dz + \frac{3z}{h^3}\int_{-h}^{h}\varepsilon_f z dz \tag{3.17}$$

where

$$\varepsilon_f = \varepsilon_s + \alpha_S \Delta T - \frac{2P}{9K} \tag{3.18}$$

Combining Equations 3.17 and 3.18 gives,

$$\varepsilon_r = \left[\left(\varepsilon_s + \alpha\Delta T\right) - \frac{1}{9hK}\int_{-h}^{h} P dz\right] + \left[\left(\varepsilon_s + \alpha\Delta T\right) - \frac{2z}{3h^3 K}\int_{-h}^{h} P z dz\right] \tag{3.19}$$

Inserting ε_r

$$\varepsilon = \frac{1+\nu}{1-\nu}\left(\varepsilon_s + \alpha\Delta T - \frac{2P}{9K}\right) + \frac{2(1-2\nu)}{(1-\nu)}\left[2\left(\varepsilon_s + \alpha\Delta T\right) - \frac{1}{9hK}\int_{-h}^{h} Pdz - \frac{2z}{3h^3K}\int_{-h}^{h} Pzdz\right] \quad (3.20)$$

Rearranging Equation 3.20 gives:

$$\varepsilon = \frac{5-7\nu}{1-\nu}\left(\varepsilon_s + \alpha\Delta T\right) - \frac{1+\nu}{1-\nu}\frac{2P}{9K} - \frac{2(1-2\nu)}{(1-\nu)}\left[\frac{1}{9hK}\int_{-h}^{h} Pdz + \frac{2z}{3h^3K}\int_{-h}^{h} Pzdz\right] \quad (3.21)$$

Taking the time derivative of ε results in:

$$\dot{\varepsilon} = \frac{5-7\nu}{1-\nu}\left(\dot{\varepsilon}_s + \alpha_S\dot{T}\right) - \frac{2}{9K}\frac{1+\nu}{1-\nu}\frac{\partial P}{\partial t} - \frac{2(1-2\nu)}{(1-\nu)}\frac{\partial}{\partial t}\left[\frac{1}{9hK}\int_{-h}^{h} Pdz + \frac{2z}{3h^3K}\int_{-h}^{h} Pzdz\right] \quad (3.22)$$

Also from Equations 3.10 and 3.11 the strain rate can be written as:

$$\dot{\varepsilon} = 3(1-\rho)\alpha_L\dot{T} + 3\alpha_S\rho\dot{T} - \frac{\partial}{\partial z}\left(\frac{D}{\eta_L}\frac{\partial P}{\partial z}\right) \quad (3.23)$$

Equating the Equations 3.22 and 3.23 gives

$$\frac{\partial}{\partial z}\left(\frac{D}{\eta_L}\frac{\partial P}{\partial z}\right) - \frac{2(1-2\nu)}{(1-\nu)}\frac{\partial}{\partial t}\left[\frac{1}{9hK}\int_{-h}^{h} Pdz + \frac{2z}{3h^3K}\int_{-h}^{h} Pzdz\right] = \frac{2}{9K}\frac{1+\nu}{1-\nu}\frac{\partial P}{\partial t} + 3(1-\rho)\alpha_L\dot{T}$$

$$+ 3\alpha_s\rho\dot{T} + \frac{5-7\nu}{1-\nu}\left(\dot{\varepsilon}_s + \alpha_s\dot{T}\right) \quad (3.24)$$

This partial differential equation for the stress in the pore liquid is derived for an unconstrained circular plate.

The boundary and initial conditions are:

$$\left.\frac{\partial P}{\partial z}\right|_{z=-h} = 0 \tag{3.25}$$

$$P|_{z=h} = 0 \tag{3.26}$$

$$P|_{t=0} = 0 \tag{3.27}$$

Since there is no liquid flow at the lower surface, the flux is zero there. At the upper surface, the stress in the liquid is zero, since it can flow freely there. Also, at time equals to zero, there is no stress in the liquid.

3.1.4. Determination of Total Stress Expression in the Plate

Free strain varies in the axial direction. The stress in axial direction is equal to zero because liquid flow is free in this direction. Hooke's Law gives the following stress-strain relationship including free strain. For the given system, only σ_r and σ_θ are considered.

$$\varepsilon_r - \varepsilon_f = \frac{1}{E}\left[-\nu(\sigma_\theta + \sigma_r)\right] \tag{3.28}$$

$$\varepsilon_\theta - \varepsilon_f = \frac{1}{E}\left[\sigma_\theta - \nu\sigma_r\right] \tag{3.29}$$

$$\varepsilon_z - \varepsilon_f = \frac{1}{E}\left[-\nu(\sigma_\theta + \sigma_r)\right] \tag{3.30}$$

The equilibrium relations in curvilinear coordinates are:

$$\frac{\partial \sigma_r}{\partial r} + \frac{1}{r}\frac{\partial \sigma_{r\theta}}{\partial \theta} + \frac{\partial \sigma_{rz}}{\partial z} + \frac{\sigma_r - \sigma_\theta}{r} = 0 \tag{3.31}$$

$$\frac{\partial \sigma_{rz}}{\partial z} + \frac{1}{r}\frac{\partial \sigma_{\theta z}}{\partial \theta} + \frac{\partial \sigma_{z}}{\partial z} + \frac{\sigma_{rz}}{r} = 0 \tag{3.32}$$

$$\frac{\partial \sigma_{r\theta}}{\partial r} + \frac{1}{r}\frac{\partial \sigma_{\theta}}{\partial \theta} + \frac{\partial \sigma_{\theta z}}{\partial z} + \frac{2\sigma_{r\theta}}{r} = 0 \tag{3.33}$$

The stresses are dependent on the length only, the surviving equation is:

$$\frac{\sigma_r - \sigma_\theta}{r} = 0 \; ; \quad \text{i.e.} \quad \sigma_r = \sigma_\theta \tag{3.34}$$

Inserting this into the Equation 3.28 gives:

$$\sigma_r = \sigma_\theta = \frac{E(\varepsilon_r - \varepsilon_f)}{1 - \nu} \tag{3.35}$$

So the total stress is equal to

$$\sigma = \frac{2E(\varepsilon_r - \varepsilon_f)}{1 - \nu} \tag{3.36}$$

ε_f is defined as

$$\varepsilon_f = \varepsilon_s + \alpha \Delta T + c'P \tag{3.37}$$

where c' is a constant which is to be determined.

Now ε_r must be determined in terms of the free strain. Stress components in an isotropic body must satisfy the six conditions of compatibility in addition to the equations of equilibrium and the boundary conditions (Boley and Weiner, 1960).

The compatibility equation used is as follows:

$$(1+\nu)\nabla^2\sigma_r + \frac{\partial^2\sigma}{\partial r^2} + \alpha E\left(\frac{1+\nu}{1-\nu}\nabla^2 T + \frac{\partial^2 T}{\partial r^2}\right) = 0 \tag{3.38}$$

Since all the variables are dependent on only z, the second and the fourth terms drop and one obtains the following differential equation:

$$\frac{d^2}{dz^2}\left(\sigma_r + \left(\frac{\alpha E}{1-\nu}T\right)\right) = 0 \tag{3.39}$$

Solving for σ_r gives

$$\sigma_r = -\frac{\alpha E}{1-\nu}T + c_1 + c_2 z \tag{3.40}$$

Using the boundary conditions;

$$\int_{-h}^{h}\sigma_r dz = \int_{-h}^{h}\sigma_r z dz = 0 \tag{3.41}$$

$$\sigma_r = \frac{\alpha E}{1-\nu}\left(-T + \frac{1}{2h}\int_{-h}^{h} T dz + \frac{3z}{h^3}\int_{-h}^{h} T z dz\right) \tag{3.42}$$

3.1.5. Determination of the Free Strain

Strains are also dependent on the stress formed in the pore liquid, P. The expressions for the strains are as follows:

$$\varepsilon_r = \frac{1}{E}\left[\tilde{\sigma}_r - \nu\left(\tilde{\sigma}_\theta + \tilde{\sigma}_z\right)\right] + cP + \alpha_S \Delta T + \varepsilon_s \tag{3.43}$$

$$\varepsilon_\theta = \frac{1}{E}\left[\tilde{\sigma}_\theta - \nu\left(\tilde{\sigma}_r + \tilde{\sigma}_z\right)\right] + cP + \alpha_S \Delta T + \varepsilon_s \tag{3.44}$$

$$\varepsilon_z = \frac{1}{E}\left[\tilde{\sigma}_z - \nu\left(\tilde{\sigma}_\theta + \tilde{\sigma}_r\right)\right] + cP + \alpha_S \Delta T + \varepsilon_s \tag{3.45}$$

where $\tilde{\sigma}$ denotes the stress on the solid. The constant c must be determined. The total volumetric strain is:

$$\varepsilon_z + \varepsilon_r + \varepsilon_\theta = \frac{1-2\nu}{E}\left[\tilde{\sigma}_z + \tilde{\sigma}_r + \tilde{\sigma}_\theta\right] + 3cP + 3\alpha_S \Delta T + 3\varepsilon_s \tag{3.46}$$

Total stress (solid and liquid), σ_k, is defined as,

$$\sigma_k = \tilde{\sigma}_k + (1-\rho)P \tag{3.47}$$

Total stress on the solid phase:

$$\tilde{\sigma}_z + \tilde{\sigma}_r + \tilde{\sigma}_\theta = \tilde{\sigma} = \sigma_r - (1-\rho)P + \sigma_\theta - (1-\rho)P + \sigma_z - (1-\rho)P \tag{3.48}$$

Since strain in the axial direction is zero, the total stress on the solid phase becomes,

$$\tilde{\sigma}_z + \tilde{\sigma}_r + \tilde{\sigma}_\theta = \tilde{\sigma} = \sigma_r - (1-\rho)P + \sigma_\theta - (1-\rho)P - (1-\rho)P \tag{3.49}$$

Volumetric strain caused by the stress on the solid and liquid part must be equal to zero as explained before.

$$\frac{\tilde{\sigma}}{3K} + 3cP = 0 \tag{3.50}$$

Bulk Modulus K is defined as:

$$K = \frac{E}{3(1-2\nu)} \tag{3.51}$$

Then stress on the solid phase is:

$$\tilde{\sigma} = \sigma - 3(1-\rho)P = 9KcP \tag{3.52}$$

The average force on the liquid is:

$$F_L = (1-\rho)\frac{F_r + F_\theta}{2} \tag{3.53}$$

Stress in the liquid is:

$$P = \frac{F_L}{(1-\rho)A} \tag{3.54}$$

Total stress is equal to: (3.55)

$$\sigma = \frac{F_r + F_\theta}{A} = 2P \tag{3.56}$$

Inserting the expression for total hydrostatic stress into equation. 3.52 gives

$$2P - 3(1-\rho)P = -9KcP \tag{3.57}$$

Then the constant c is equal to.

$$c = \frac{1-3\rho}{9K} \tag{3.58}$$

The equations are written in terms of total stresses instead of stresses on the solid are:

$$\frac{1}{E}\left[\tilde{\sigma}_r - \nu\left(\tilde{\sigma}_\theta + \tilde{\sigma}_z\right)\right] + cP = \frac{1}{E}\left[-(1-\rho)P - 2\nu\left(\sigma_r - (1-\rho)P\right)\right] + \frac{1-3\rho}{9K} \tag{3.59}$$

$$\frac{1}{E}\left[\tilde{\sigma}_r - \nu\left(\tilde{\sigma}_\theta + \tilde{\sigma}_z\right)\right] + cP = -\frac{2\nu\sigma_r}{E} - \frac{2P}{9K} \tag{3.60}$$

Free strain is,

$$\varepsilon_f = \varepsilon_s + \alpha_S \Delta T - \frac{2P}{9K} \tag{3.61}$$

3.1.6. Effect of Radial Constraint

Radial constraint represents the walls of the container. It prevents flow and expansion in the radial direction. Since expansion in the radial direction is prevented, $\varepsilon_r = \varepsilon_\theta = 0$. Flow is in the axial direction and the expansion in the axial direction is free. Therefore, stress in this direction is zero.

Strains in terms of free strain and total stresses are,

$$\varepsilon_r - \varepsilon_f = \frac{1}{E}\left[\sigma_r - \nu\left(\sigma_\theta + \sigma_z\right)\right] \tag{3.62}$$

$$\varepsilon_\theta - \varepsilon_f = \frac{1}{E}\left[\sigma_\theta - \nu\left(\sigma_r + \sigma_z\right)\right] \tag{3.63}$$

$$\varepsilon_z - \varepsilon_f = \frac{1}{E}\left[\sigma_z - \nu\left(\sigma_r + \sigma_\theta\right)\right] \tag{3.64}$$

Expressing the strain in the radial direction in terms of total stress and free strain gives:

$$\varepsilon_r = \frac{1}{E}\left[(1-\nu)\sigma_r\right] + \varepsilon_f \tag{3.65}$$

Since radial strain is equal to zero, the radial stress is:

$$\sigma_r = -\frac{\varepsilon_f E}{(1-\nu)} \tag{3.66}$$

Strain in the z direction becomes:

$$\varepsilon_z = \frac{\varepsilon_f(1+\nu)}{(1-\nu)} \tag{3.67}$$

In case of radial constraint, strain in the z direction becomes three times larger than when the gel expands in three dimensions.

$$\varepsilon = 3\frac{\varepsilon_f(1+\nu)}{(1-\nu)} \tag{3.68}$$

Inserting the expression for free strain, then differentiating with respect to time gives:

$$\dot{\varepsilon} = \frac{1+\nu}{1-\nu}\left(3\dot{\varepsilon}_s + 3\alpha_S\dot{T} - \frac{2}{3K}\frac{\partial P}{\partial t}\right) \tag{3.69}$$

Rewriting Equation 3.23, one obtains:

$$\dot{\varepsilon} = 3(1-\rho)\alpha_L\dot{T} + 3\alpha_S\dot{T} - \frac{D}{\eta_L}\frac{\partial^2 P}{\partial z^2} \tag{3.23}$$

Equating Equations 3.23 and 3.69 gives

$$\frac{D}{\eta_L}\frac{\partial^2 P}{\partial z^2} = \left(\frac{1+\nu}{1-\nu}\right)\frac{2}{3K}\frac{\partial P}{\partial t} + \left(\frac{-2\nu}{1-\nu}\right)3\alpha_S\dot{T} + 3(1-\rho)\alpha_L\dot{T} - \left(\frac{1+\nu}{1-\nu}\right)3\dot{\varepsilon}_s \qquad (3.70)$$

The boundary conditions are:

$$\left.\frac{\partial P}{\partial z}\right|_{z=0} = 0 \qquad (3.71)$$

$$P|_{z=h} = 0 \qquad (3.26)$$

$$P|_{t=0} = 0 \qquad (3.27)$$

The partial differential equation is used to find the change in stress in the liquid with changing temperature. Radial stress is found from stress in the liquid. Then it is compared with the modulus of rupture of the gel-network to decide whether the gel will crack or not during heating.

3.2. Solution Methods

Partial differential equation derived by modeling the system with radial constraint is solved using computer software packages.

3.2.1. PDECOL

PDECOL consists of a collection of 19 subroutines written in standard Fortran (Madsen, Sincovec, 1979). It is designed to solve the general system of NPDE, nonlinear partial differential equations of at most second order on the interval [x_L ,x_R] for $t \geq t_0$ which is of the form

$$\frac{\partial u}{\partial t} = f\left(t, x, u, u_x, u_{xx}\right) \tag{3.72}$$

where

$$u = \left(u_1, u_2 \ldots\ldots\ldots, u_{NPDE}\right)$$

$$u_x = \left(\frac{\partial u_1}{\partial x}, \frac{\partial u_2}{\partial x}, \ldots\ldots \frac{\partial u_{NPDE}}{\partial x}\right) \tag{3.73}$$

$$u_{xx} = \left(\frac{\partial^2 u_1}{\partial x^2}, \frac{\partial^2 u_2}{\partial x^2}, \ldots\ldots \frac{\partial^2 u_{NPDE}}{\partial x^2}\right)$$

Depending on the particular type of equation, 0, 1, or 2 boundary conditions may be required for each equation in the system 3.72. These are imposed at x_L and/or x_R and must be of the form

$$b(u, u_x) = z(t) \tag{3.74}$$

where b and z are arbitrary vector valued functions with NPDE components.

Each solution component u_k is assumed to be a known function of x at the initial time $t=t_0$.

$$u_k(t_0, x) = \phi_k(x), \qquad k = 1,2,\ldots\ldots\ldots NPDE \tag{3.75}$$

where each $\phi_k(x)$ is a known function of x. The initial condition functions must be consistent with the boundary conditions.

The PDE system described is completely specified if NPDE, the interval $[x_L, x_R]$; the initial time t_0, the vector functions f, b, and z, and the initial condition functions ϕ_k are given.

The user is required to construct three subroutines that specify the form of PDE problem. These are F, BNDRY and UINIT. For given input values of t and x and corresponding input values of u, u_x and u_{xx} which are associated with this time and spatial position, subroutine F is to compute appropriate values for for the functions f_k, subroutine BNDRY is to compute values for the derivatives of the boundary condition functions b_k and z_k.. subroutine UINIT is to compute the initial condition function values.

PDECOL is based on method on lines and it uses a finite element collocation procedure (with piecewise polynomials as the trial space) for the discretization of the spatial variable x. The collocation procedure reduces the PDE system to a semidiscrete system (an initial value ODE system) that depends only on the time variable t.

The basic assumption made is that any given time t, each approximate solution component, u_k, is a piecewise polynomial in the user defined space and can be written in terms of basis functions as

$$u_k(t,k) = \sum_{i=1}^{NCPTS} c_{i,k}(t)\,\phi_i(x), \qquad k = 1,2,.....NPDE \tag{3.76}$$

Number of piecewise polynomials, NCPTS is given by the user. The unknown coefficients $c_{i,k}$ depend on the time t, and the known basis functions ϕ_i depend on x. The semi discrete equations (ordinary differential equations) which determine these coefficients $c_{i,k}$, for i=1,2,....., NCPTS and k= 1,2, ...NPDE, are obtained by collocating, by requiring the approximate u_k (t,x) to satisfy the PDE's and the boundary conditions exactly, at a set of NCPTS collocation points.

NCPTS collocation points are chosen such that

$$x_L = \xi_1 < \xi_2 < \ldots\ldots\ldots\ldots \xi_{NCPTS} = x_R \tag{3.77}$$

Substituting Equation 3.76 into 3.72 and requiring Equation 3.72 to be valid at the interior collocation points gives

$$\sum_{i=1}^{NCPTS} \phi_i(\xi_j)\frac{dc_{i,k}}{dt} = f_k\left(t,\ \xi_j,\ u(t,\xi_j), u_x(t,\xi_j), u_{xx}\ (t,\xi_j)\right), \qquad (3.78)$$

$$j = 2,3,.....NCPTS-1, \quad k = 1,2,.....NPDE.$$

To determine the equations corresponding to j=1 and j=NCPTS, equations that depend on the type of boundary conditions are formed. An ODE corresponding to the point $x=x_L$ is formed by differentiating the boundary condition.

$$\sum_{j=1}^{NPDE}\left\{\frac{\partial b_k}{\partial u_j}\frac{\partial u_j}{\partial t} + \frac{\partial b_k}{\partial u_{x_j}}\frac{\partial u_{x_j}}{\partial t}\right\} = \frac{dz_k}{dt} \qquad (3.79)$$

Substituting Equation 3.76 into 3.78 and using the facts that

$$\phi_1(x_L) \neq 0$$
$$\phi_i(x_L) = 0 \qquad i = 2,3,.....NCPTS$$
$$\phi_1'(x_L) \neq 0$$
$$\phi_2'(x_L) \neq 0$$
$$\phi_i'(x_L) = 0 \qquad i = 3,4,.....NCPTS$$

gives the appropriate ordinary differential equations

$$\sum_{j=1}^{NPDE}\left\{\frac{\partial b_k}{\partial u_j}\phi_i(x_L) + \frac{\partial b_k}{\partial u_{x_j}}\phi_1'(x_L)\right\}\frac{dc_{1,j}}{dt} + \sum_{j=1}^{NPDE}\left\{\frac{\partial b_k}{\partial u_{x_j}}\phi_2'(x_L)\right\}\frac{dc_{2,j}}{dt} = \frac{dz_k}{dt} \qquad (3.80)$$

Combining the boundary condition equations with Equation 3.78 yields a semidiscrete system of N= NPDE·NCPTS time dependent ordinary differential equations that have the form

$$A\frac{dc}{dt} = g(t,c) \qquad (3.81)$$

The methods used to advance the time are based on multipoint formulas of the form

$$c_n = \sum_{j=1}^{k_1} \alpha_j c_{n-j} + \Delta t \sum_{j=0}^{k_2} \beta_j c'_{n-j} \tag{3.82}$$

here, c_k is the approximation to the exact value at $t=t_k$ and α_j and β_j are the method coefficients. Since $\beta_0 \neq 0$ for the methods used, the time integration methods are implicit and in general a nonlinear system of equations must be solved for every time step taken.

3.2.2. PDEase2D

PDEase2D is a general purpose computer program for obtaining numerical solutions to many classes of steady-state boundary value, time dependent boundary value, initial value and eigen value problems. PDEase2D uses the Galerkin Finite Element Method of Weighted Residuals with quadratic basis to convert continuos partial differential equations into discrete nodal equations. This method ensures accurate results and rapid convergence.

PDEase2D starts with a coarse grid of triangular patches. It then uses an iterative process to refine the grid. As each iteration is completed, PDEase2D determines the error in each patch and subdivides only the patches where the error exceeds a default or user specified error limit.

In the method of weighted residuals, it is given a differential operator L and a function f(x) on a region V satisfying:

$$L(f(x))=0 \tag{3.83}$$

Then for any function W(x),

$$\int_V W(x)L(F(x))dx = 0 \tag{3.84}$$

If it is given any function g(x), then

$$\int_V W(x)L(g(x))dx \equiv R \tag{3.85}$$

is a measure of the residual error involved if g(x) is used as an approximate solution of L(f(x))=0. The shape of the weight function W(x) determines the weighting of the error at each point x in the region V.

The static Heat Equation is taken as an example. The differential equation to be solved on a region V:

$$KTemp(x) + Source(x) = 0 \tag{3.86}$$

where

K= (constant) thermal conductivity
Source(x)= heat source as a function of position(x)
Temp(x)=temperature distribution as a function of position(x)

The boundary conditions on the boundary V are convective:

$$-KTemp_{norm} = K_b\left(Temp(x) - Temp_b(x)\right) \tag{3.87}$$

where

$Temp_{norm}$ = outward normal derivative on the boundary of the region V
$Temp_b(x)$ = bath temperature as a function of position on the boundary of V
K_b = (constant) thermal conductivity of the boundary

A finite set of basis functions $\left(N_\alpha(x) \middle| \alpha = 1,\ldots\ldots,\text{Nbasis}\right)$ is defined on the region V, and all functions on V are approximated as linear combinations of these functions.

The differential equation is represented as linear combinations of the basis functions $N_\beta(x)$

$$KN_\beta(x)^j \ \text{Temp}^\beta + N\beta(x) \ \text{Source}^\beta = 0 \tag{3.88}$$

According to The Method of Weighted Residuals

$$-\int_V W(x)^j \ N_j \text{Temp}\, dx + \oint_V W(x)N(x)\text{Temp}_b - \text{Temp} + \int_V W(x)N(x)\text{Source}dx = 0 \tag{3.89}$$

There are as many unknown coefficients Temp^β as there are basis functions. There are as many residual error equations as there are weight functions. If the same number of weight and basis functions is chosen, then the same number of equations are obtained as there are unknowns. If the functions are properly chosen, this system has a unique solution.

Galerkin Method is a special case of the Method of Weighted Residuals. It uses the same functions as basis functions and weight functions.

A special case of Galerkin Method is the Finite Element Method. In this method, the basis/weight functions are C^0 functions which are piecewise polynomials with very localized support. The support of a function is the subregion of its domain where the function takes on nonzero values.

It is assumed that the region V is a manifold with boundary of dimension DIM. If DIM=2, then V is a plane region and it is represented by triangles in finite element method. Linear functions are defined in this triangulated region. The finite element method usually employes functions which are low degree piecewise polynomials, when expressed in the affine coordinates in each element. Smaller, more numerous elements can be used in subregions where it is desired to approximate the solution function more closely.

3.2. Properties of the Silica Gel-Network

Table 2.3. shows the properties of silica and the pore liquid methanol which are used to determine stress development in a cylindrical gel of high thickness. Viscosity and thermal expansion coefficient are dependent on the temperature (Scherer, 1992)

Table 3.1. Properties of the Silica Gel-Network

Properties	**Symbols**	**Values**
Poisson Ratio	ν	0.2
Young's Modulus	E	$12\ 10^6$ Pa
Bulk Modulus	K	$6.67\ 10^6$ Pa
Volumetric Solid Fraction	ρ	0.1
Permeability	D	$5\ 10^{-18}$ m^2
Critical Temperature	T_c	240 °C
Thermal Expansion Coefficient	α_L	$0.0263(T_c\text{-}T)^{-0.768}$ (°C^{-1})
Liquid Viscosity	η_L	$(51.9/T(K))^{4.29}$ (Pa·s)

Syneresis of the gel network is presented by the following function.

$$\varepsilon_s = \varepsilon_s^{\infty}\left[1-\exp\left(-\int_0^t \frac{dt'}{\tau_s(t')}\right)\right] \tag{3.90}$$

The characteristic time has an Arrhenius temperature dependence.

$$\tau_s = \tau_0 \exp\left(\frac{Q_s}{RT}\right) \tag{3.91}$$

ε_s^{∞} represents the maximum shrinkage of the network due to syneresis. For silica gel, it is fifteen percent. The activation energy and the characteristic time constant for syneresis are given as follows (Scherer, 1992):

$\varepsilon_s^{\infty} = -0.15$ and $Q = 10$ kcal / mole and $\tau_0 = 0.01$ s.

The integral in the Equation 3.90 is evaluated by Simson's Rule. The rate of syneresis is found by using five point differentiation formula.

4. RESULTS AND DISCUSSION

In this study, stress development in a porous structure during heating step of supercritical drying is modeled. The originality of the work comes from the geometry of the gel network which is a circular plate. Also, model equations are developed for the circular plate which has radial constraint. The application of this model to a cylinder of high thickness is acceptable since the radial flow is already prevented by the radial constraint. Therefore, the partial differential equation is both applied to a cylinder of high thickness and a circular plate. In the former, the properties of silica gel of similar geometry are taken and in the latter, the properties are varied for a theoretical gel network.

4.1. Cylindrical Silica Gel

Stress development during heating to reach supercritical conditions is modeled for a cylindrical gel of high thickness by Scherer (see section 2.5.1.). In the study, the cylindrical gel has no constraints. Accounting for the high thickness to radius ratio, axial flow is less important than the radial flow and it is neglected. The model equation derived is dependent on the radius and the most significant stresses develop in the axial direction. The axial stress is computed for different heating rates and shear moduli. Also, the same computations are done for the presence of syneresis. The magnitudes of the stresses formed are compared with the modulus of rupture of the network to determine whether the gel will crack.

In the present study, the model equation for the heating step is derived for a circular plate. Then the model equation is manipulated for the case of radial constraint. Actually, the difference between a circular plate and a cylinder disappears when a radial constraint is applied. Since there is a radial constraint, the pore liquid can escape from the network only in the axial direction and the model equation is dependent on thickness rather than radius. Radial constraint prevents radial expansion of the gel network. On the other hand, the network is free to expand in the axial direction. Also the liquid flows in the axial direction.

Therefore, the most significant stresses form in the radial direction. In case of a circular plate, stress in the axial direction is zero while for a cylinder with radial constraint, the axial stress is neglected in comparison to the radial stress.

Partial Differential Equation derived for the case with radial constraint is first solved neglecting the presence of syneresis. For a cylindrical gel of 18 cm. thickness, inserting a radial constraint and preventing radial flow and radial expansion, brings a significant change in the magnitude of the stress formed. The stress in the liquid increases as the liquid expands, and stretches the network. The network applies a compressive stress on the liquid which makes it flow. The maximum stress in the liquid (at about 200 °C) is in the order of 3 MPa when the heating rate is 2 °C/min. The magnitude does not change much when the rates are reduced to 1 °C/min and 0.5 °C/min. (Figure 4.1). Viscosity and thermal expansion coefficient are temperature dependent. As temperature increases, viscosity decreases. On the other hand, thermal expansion coefficient increases with increasing temperature. Because the coefficient of the second spatial derivative of stress is too small due to high thickness, the increase in the contribution of thermal expansion term and the decrease of viscosity with temperature do not shift the curves.

Stress development along the thickness of the cylinder decreases with decreasing heating rate (Figure 4.2). Since there is no flow at the lower surface, maximum stress forms there and the stress in the upper surface is zero as the boundary condition states.

The radial stress shows the same kind of behavior with the stress in the liquid (Figure 4.3). The order of magnitude of stress formed is about 1.5 MPa. This is comparable with the modulus of rupture of the network which is 0.2 MPa in the alcogel and it increases to 2MPa in the aerogel (Scherer, 1992). The stress formed is lower than the modulus of rupture. Also the maximum stress is formed at high temperatures when the modulus approaches its value measured in aerogel.

Figure 4.4 shows the change in radial stress with thickness. Radial stress decreases toward the upper surface as the stress in the pore liquid The shear modulus G of the alcogel is measured as five MPa. This value increases to 100 MPa for the aerogel. Since functional

form of shear modulus is not known, different values are assumed and stress is calculated as a function of temperature for different values of shear modulus to observe its effect. Stress development increases with increasing shear modulus. The reason can be explained with the fact that for a given strain, stress formation is higher in the material that has a higher modulus. Therefore, when the liquid tries to expand, the network of higher modulus applies more severe compressive stresses on the liquid. Change in stress development with shear modulus is also examined in the study of Scherer (Scherer, 1992). The general behavior is that the stress increases as the liquid stretches the network to expand (Figure 4.6). As a response, the network applies compressive stress on the liquid and causes the pore liquid to flow out of the network. The viscosity of the liquid is temperature dependent, it decreases with increasing temperature and this accelerates the liquid flux. Therefore, stress has a maximum.

The behavior observed in the case of radial constraint is entirely different. The decrease in the viscosity and the increase in the liquid flux are not able to decrease stress formation when radial constraint is applied. Instead, the stress increases steadily (Figure 4.5). In the study of Scherer, it is expressed that the curve for G= 5 MPa is more realistic and the rapid increase observed in the the curve for G= 100 MPa does not occur in practice. Comparing the curves for G= 5 MPa suggests that stress formation is about ten times greater when the gel is bounded radially. Morover, as the temperature increases, the stress curves for higher moduli begin to represent the system (Figure 4.5). Therefore, the stresses formed in two cases must differ more then ten fold.

The presence of syneresis must be taken into account for a more realistic modeling. In the study of Scherer, the properties measured are of a cylindrical gel hydrolyzed at neutral conditions (Scherer, 1992). This kind of gels exhibit stronger syneresis in comparison to the base catalyzed silica gels. Syneresis completes in about ten days at room temperature and the gel shrinks about 15 percent. Actually, when the gel shrinks, the system looses the radial constraint condition. Therefore, using the properties of base catalyzed gels which exhibit less syneresis is better when modeling the case with radial constraint and syneresis. Since only the properties of the gel hydrolyzed at neutral conditions are given, they are used in the

present model. Also, shrinkage of the network can be overcome by thermal expansion which makes the gel come into contact with the container wall.

The partial differential equation including syneresis strain rate is solved (Equation 3.70). The curves for stress in the liquid, P, and radial stress σ_r are similar again (Figure 4.7 and Figure 4.9). When syneresis is not taken into account, there is not much difference between the curves for heating rates of 0.5 °C/min, 1 °C/min, and 2 °C/min as discussed before (Figure 4.1 and Figure 4.3). Syneresis brings a significant change in the behavior of stress development. The curves have maxima when syneresis has the fastest rate. Syneresis completes at about 140 °C for 0.5 °C/min while it completes at about 180 °C for 2 °C/min (Figure 4.15). Therefore syneresis curve for a heating rate of 0.5 °C/min gets steeper at a lower temperature than the one for a heating rate of 2 °C/min and this is the reason for the larger stresses observed for 0.5 °C/min at temperatures below 140 °C.

In Figure 4.9, it can also be seen that the stresses exceed 2 MPa, the modulus of rupture of aerogel, at low temperatures. Therefore, the gel can probably not stand the stress formed and it will crack which makes producing monoliths at this heating rates impossible. On the other hand, stresses do not exceed the limit when there is no constraint (Figure 4.10).

Stress development at different shear moduli is also examined for the case with syneresis (Figure 4.11). The magnitudes of stresses begin to decline when syneresis strain rate decreases. This occurs at about 160 °C. The stress for the case where there is no constraint (Figure 4.12) is an order of magnitude less in comparison to the stress in gel with radial constraint for flow.

Since stresses formed exceed the modulus of rupture at the heating rates studied (0.5 °C/min - 2 °C/min), the effect of heating rate is is investigated at lower rates (0.05 °C/min and 0.04 °C/min) (Figure 4.13). When syneresis is neglected, it is observed that the curves start resembling to the ones computed for the case of no constraint (Figure 4.6). The radial stress starts from zero and increases with temperature as the expanding pore liquid stretches the network. Instead of a steady increase in the magnitude, the rate of stress formation decreases because viscosity decreases with increasing temperature. At low heating rates,

pore liquid can find time to escape from the network. When syneresis is included, two maxima occur (Figure 4.14). First is due to syneresis. Second is related to the increase in the liquid flux. When syneresis is allowed for, the magnitudes of stresses are above two MPa limit at low temperatures. Actually, these heating rates are not of physical significance. At the heating rate of 0.04 °C/min, it takes about 4 days to reach critical conditions, which results in aging of the gel.

Syneresis strains are shown at different heating rates in Figure 4.15 and Figure 4.16. Since, syneresis is time dependent, maximum syneresis strain rates are arrived at higher temperatures for higher heating rates.

4.2. Circular Plate

The same partial differential equation is solved to see the effect of thickness in the stress formation for a circular plate. Since the properties for a gel of low thickness are not known, the parameters are varied. Also, syneresis could not be taken into consideration because of the lack of an appropriate syneresis function.

At heating rates of 0.5 °C/min, 2.0 °C/min and 5.0 °C/min , the stresses formed in the liquid and in the network are in the order of 1000 Pa, which is low in comparison to a high thickness cylinder. On the other hand, modulus of rupture must also be lower for a plate. It is observed that, the magnitudes of stresses increase very much with increasing heating rates when compared to the cylinder (Figure 4.17, Figure 4.19).

The stress in the pore liquid takes its maximum value at the lower surface and it is zero at the upper surface in accordance with the boundary conditions (Figure 4.18).

The strain formed under these stresses are also computed this time since the modulus of rupture is not known and there is no information about crack formation. Strain curves show the same characteristics with the stress curves. As stress increases, the strain also increases.

Since the liquid flux out of the network increases at higher temperatures, stress as well as instantaneous strain decrease (Figure 4.20).

The permeability of the network is varied to observe its effect on stress formation (Figure 4.21). According to Darcy's Law, liquid flux decreases with decreasing permeability. Therefore, at lower permeabilities, stress formation is more.

High heating rates are also examined (Figure 4.22). At a heating rate of about 1000 °C/min which is chosen to represent flash heating, the magnitude of maximum stress exceeds 2.5 MPa which is even higher than the modulus of rupture for the cylinder of high thickness. Therefore, it can be concluded that cracking is inevitable at that heating rate for the circular plate.

Shear modulus is also varied for the circular plate (Figure 4.23 and Figure 4.24). The magnitude of stress formed doesn't change significantly with increasing G. For a body of low thickness which can expand in one direction, change in shear modulus doesn't bring extra stress formation contrary to the increase in stress formation brought by higher heating rates.

Finally, to make a comparison, the partial differential equation is solved by PDEase2D for the case of a circular plate heated at a rate of 2 °C/min. The curves show the same trend and the numerical values are similar. It is not observed that much difference in the magnitudes of stresses due to solution technique. The magnitudes of maximum stresses computed by PDECOL and PDEase2D are the same which is about 2000 Pa. (Figure 4.25 and Figure 4.26).

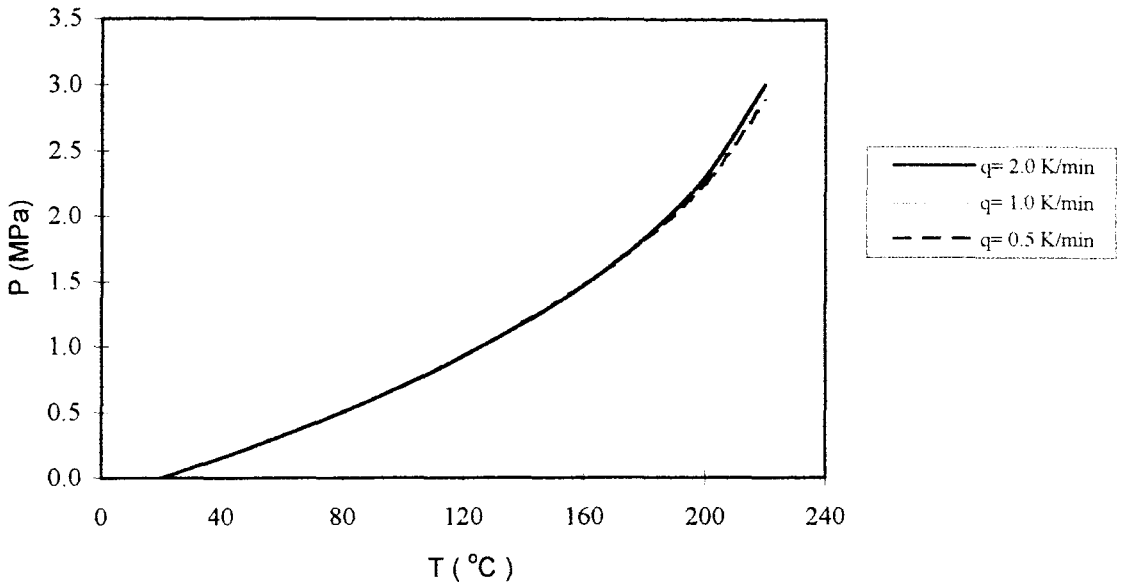

Figure 4.1. Change in stress in the pore liquid with temperature at different heating rates for a thickness of 18 cm (G=5MPa).

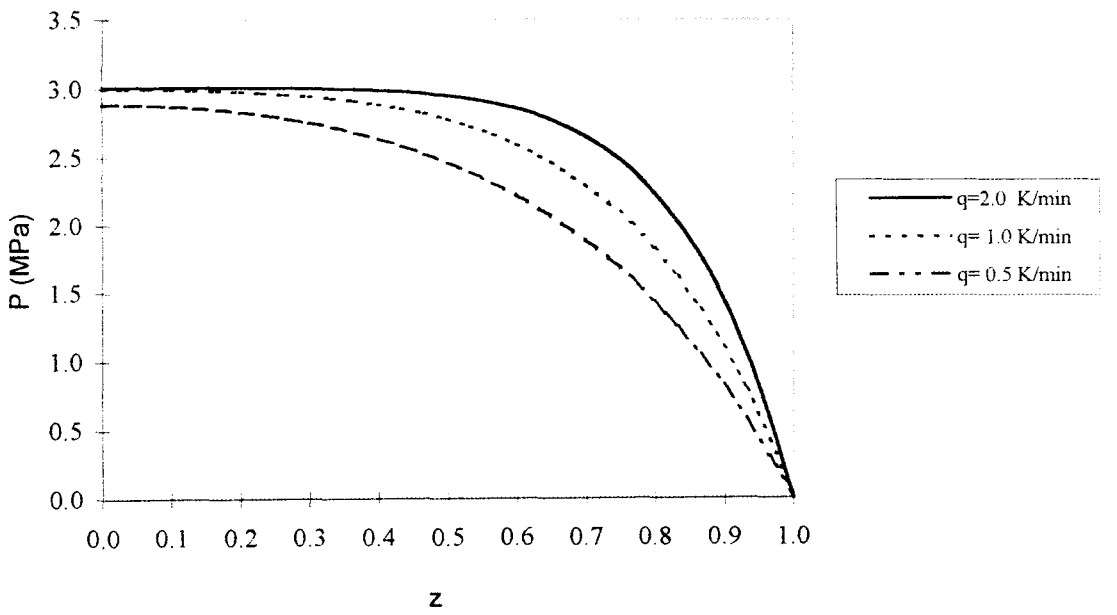

Figure 4.2. Change in stress in the pore liquid with thickness at a temperature of 220 °C at different heating rates (G= 5MPa).

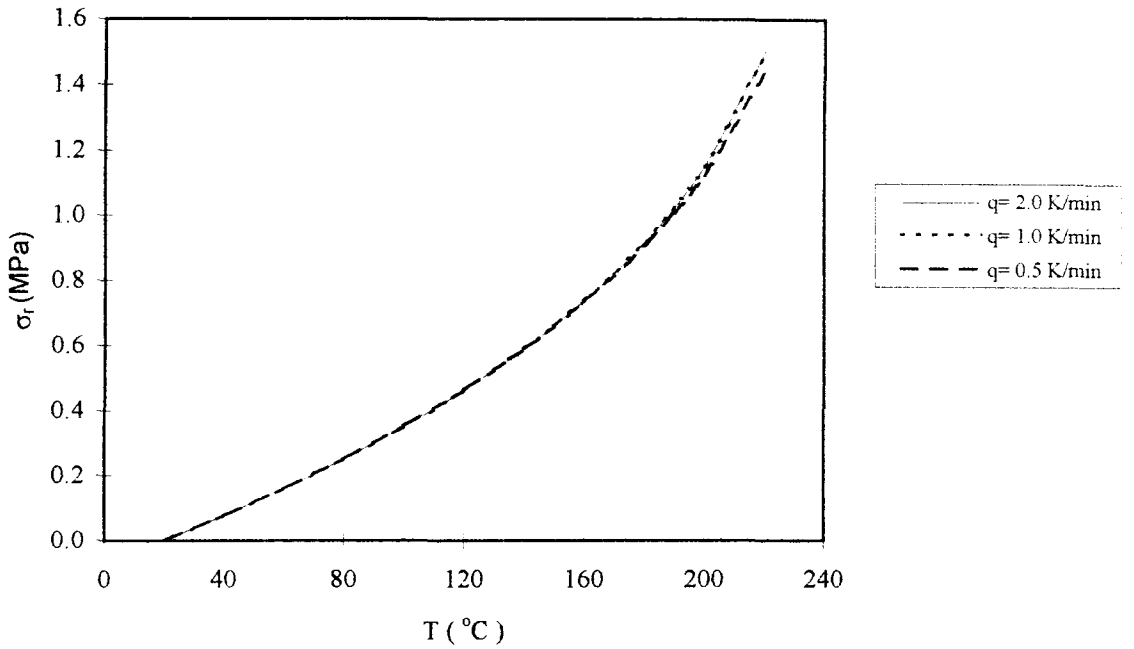

Figure 4.3. Change in radial stress with temperature at different heating rates at a thickness of 18 cm (G=5.MPa).

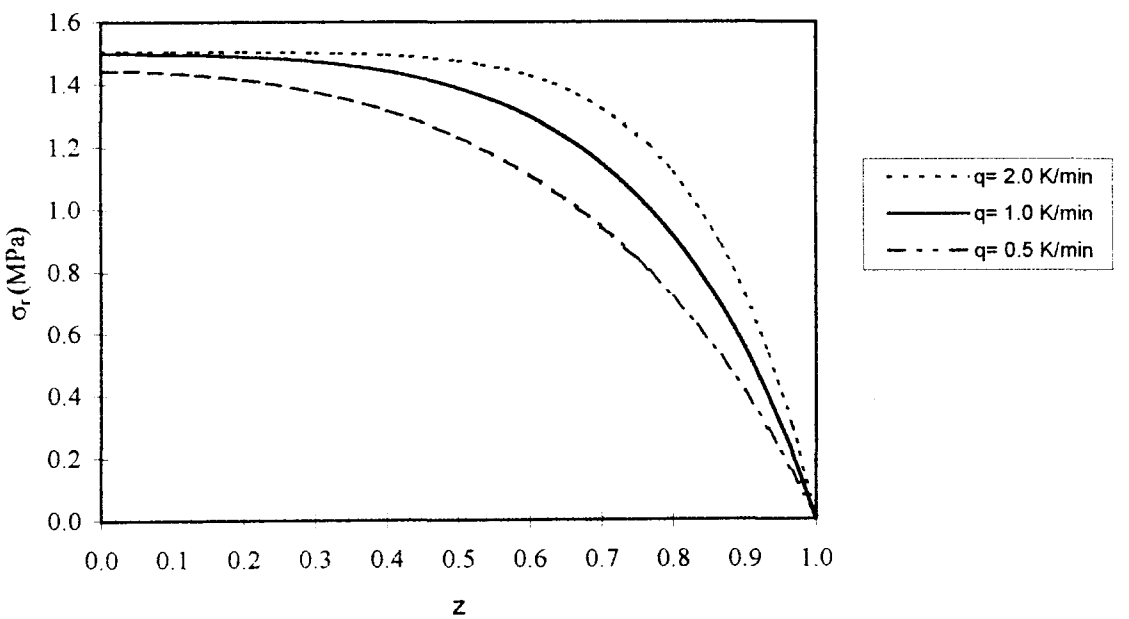

Figure 4.4. Change in stress in the pore liquid with thickness at different heating rates at a temperature of 220 °C.

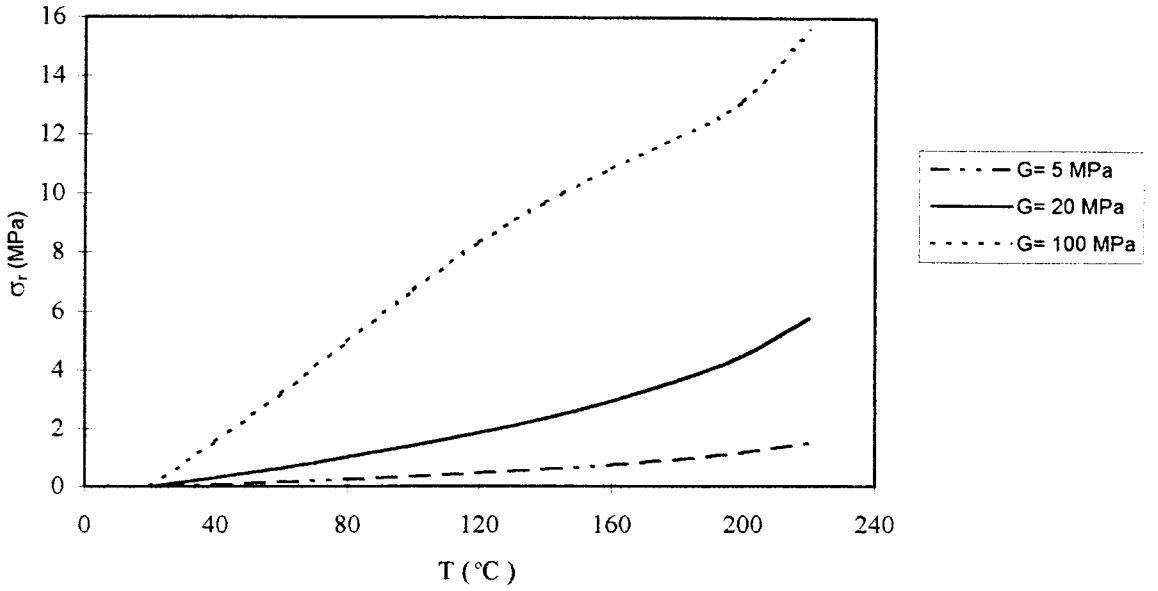

Figure 4.5. Change in radial stress with temperature for different shear moduli at a heating rate of 2.0 °C/min (h=18cm).

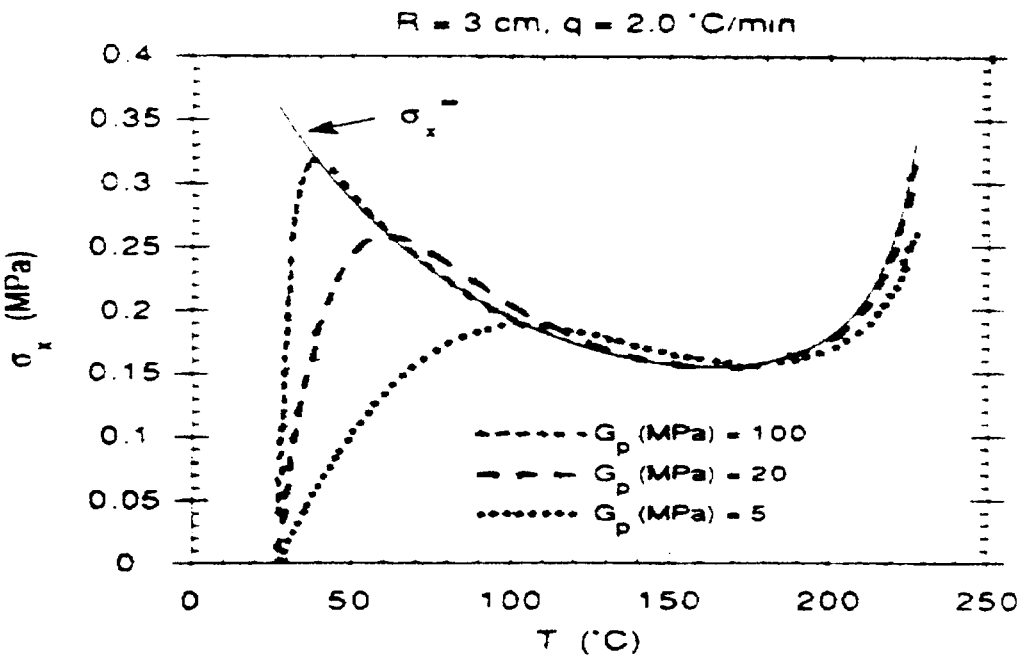

Figure 4.6. Change in axial stress with temperature for different shear moduli at a heating rate of 2.0 °C/min (h =18 cm), (Scherer, 1992).

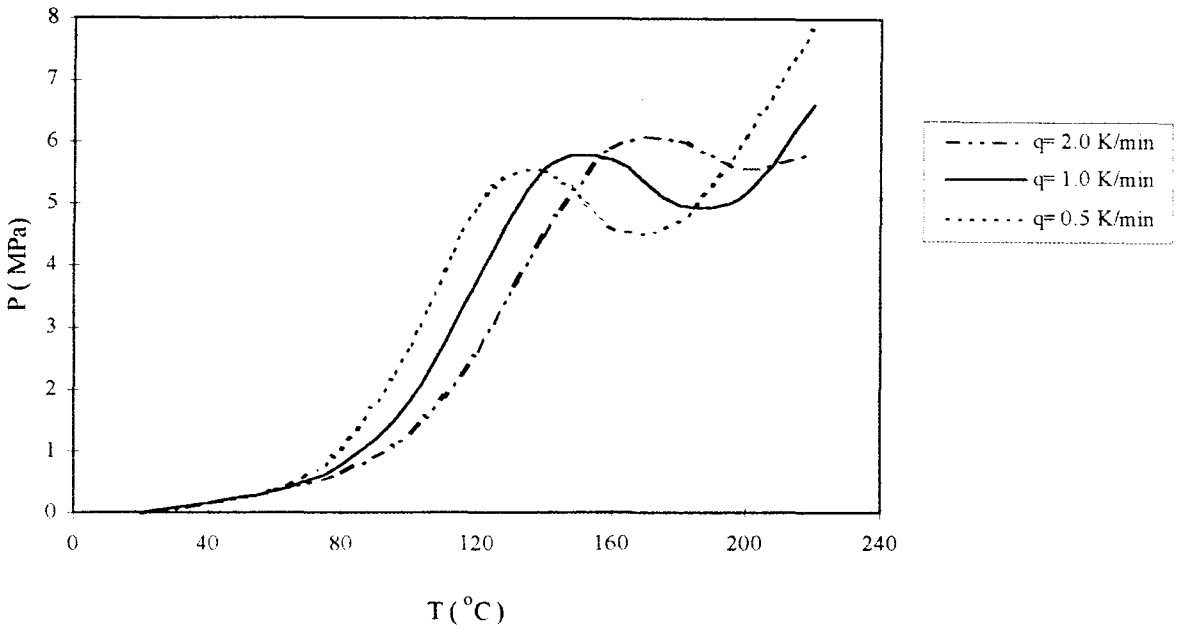

Figure 4.7. Change in stress in the pore liquid with temperature at different heating rates at a thickness of 18 cm. when syneresis is included (G=5 MPa).

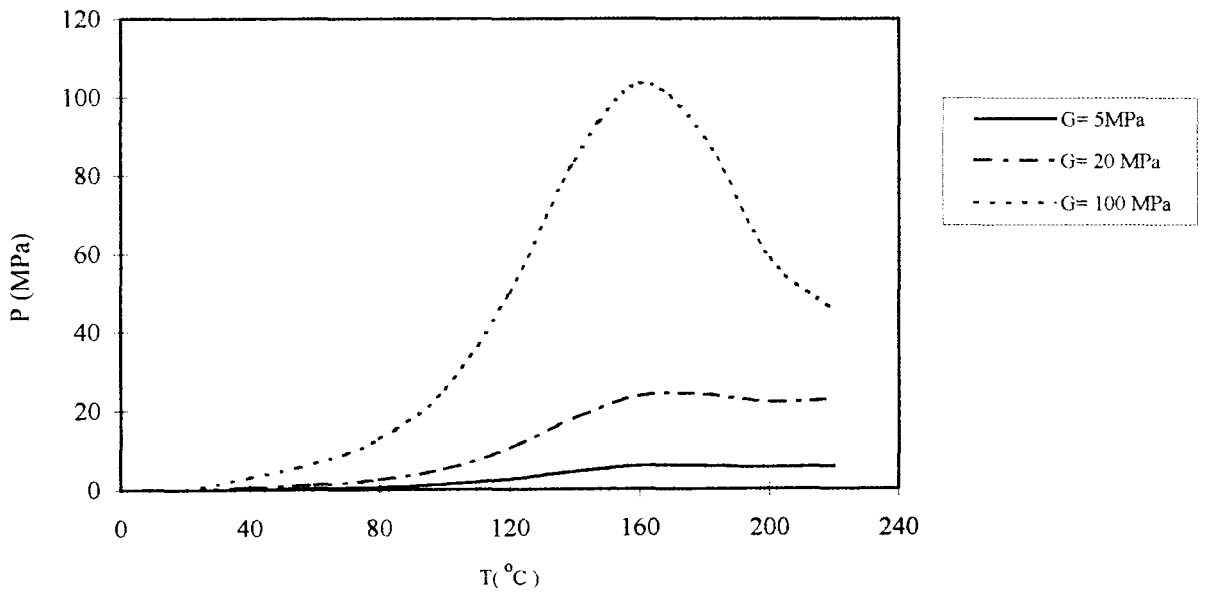

Figure 4.8. Change in the stress developed in the pore liquid with temperature at different shear moduli when syneresis is included for a heating rate of 2.0 °C/min.

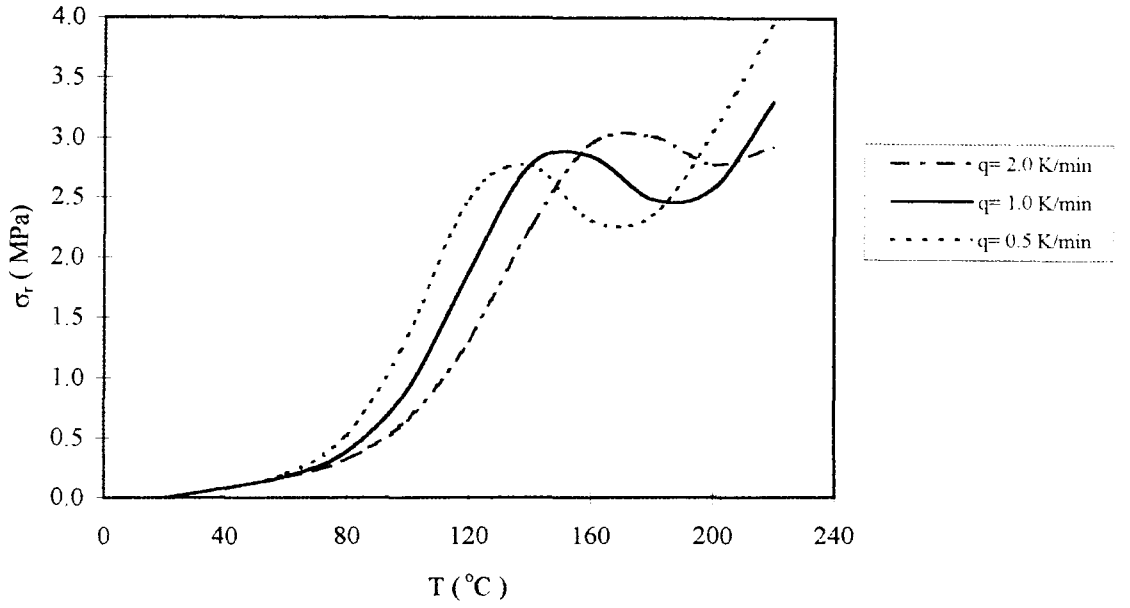

Figure 4.9. Change in radial stress with temperature at different heating rates at a thickness of 18 cm. when syneresis is included (G=5 MPa).

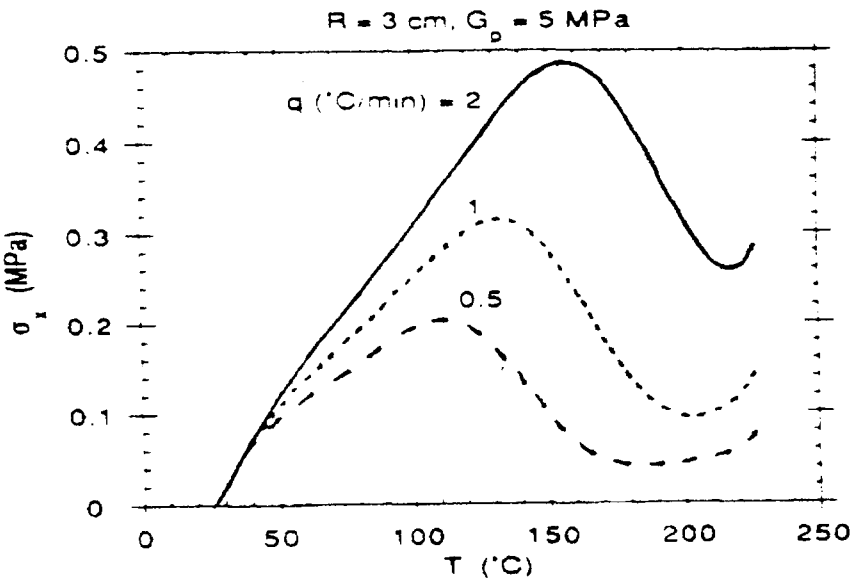

Figure 4.10. Change in radial stress with temperature at different heating rates at a thickness of 18 cm. when syneresis is included (G=5 MPa), (Scherer, 1992).

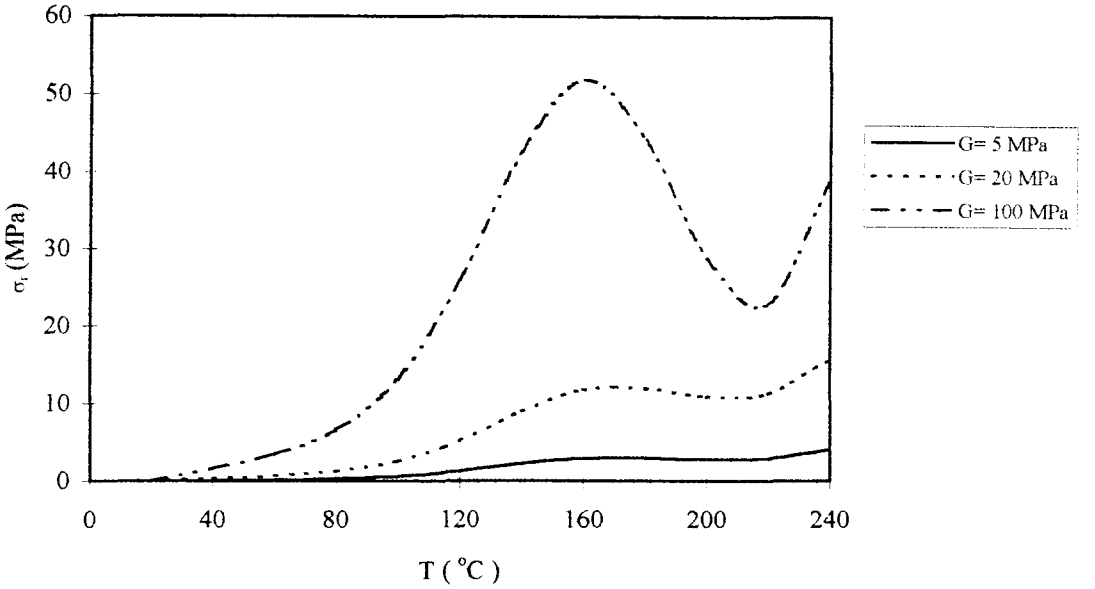

Figure 4.11. Change in radial stress with. temperature at different shear moduli at a thickness of 18 cm. allowing for syneresis.

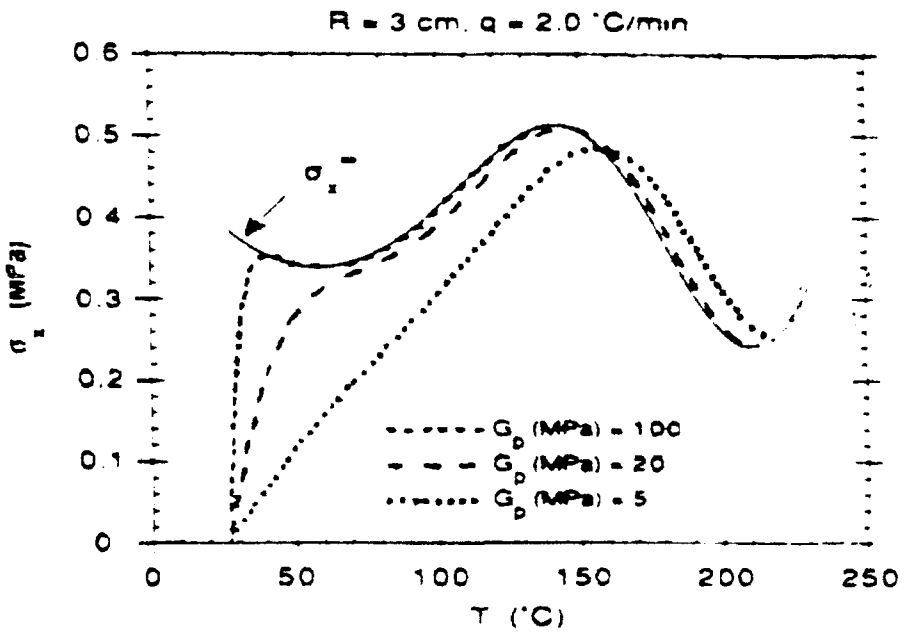

Figure 4.12. Change in the axial stress with temperature at different shear moduli when syneresis is included for a heating rate of 2.0 °C/min (Scherer, 1992).

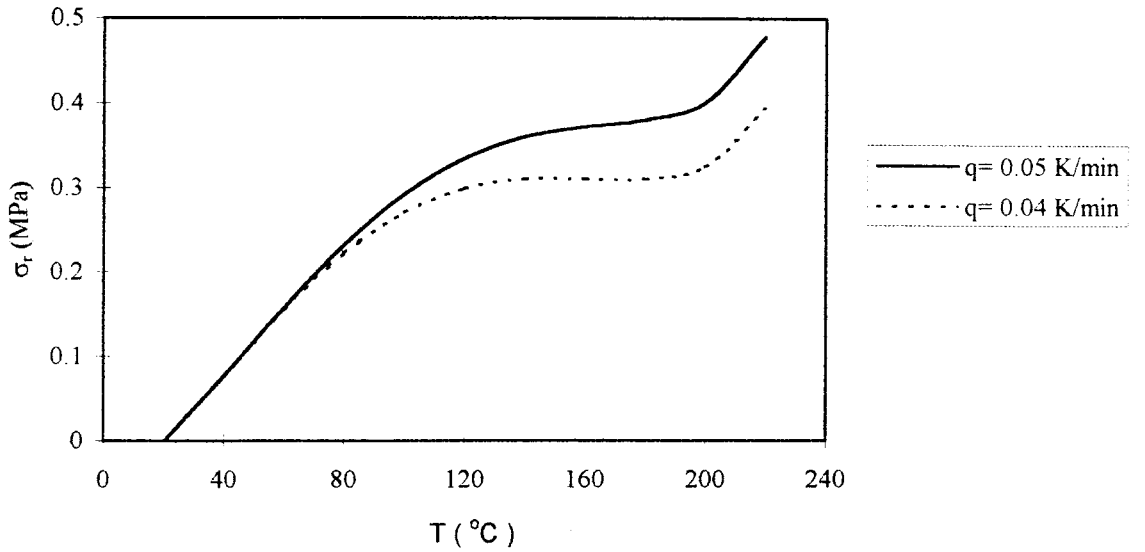

Figure 4.13. Change in stress in the pore liquid with temperature at different heating rates for a thickness of 18 cm (G= 5MPa).

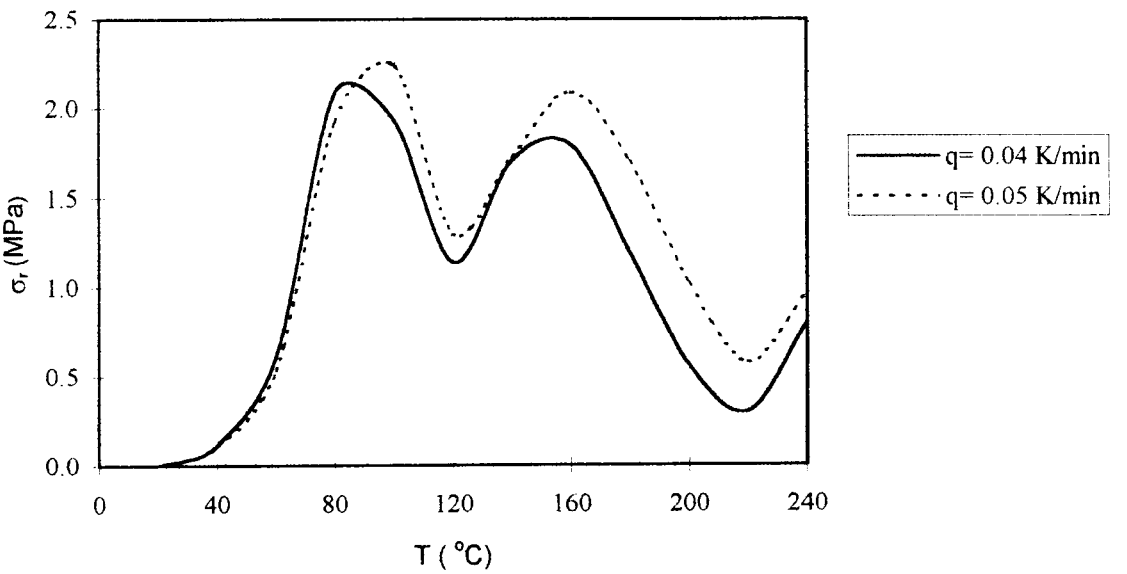

Figure 4.14. Change in stress in the pore liquid with temperature at different heating rates for a thickness of 18 cm allowing for syneresis (G= 5MPa).

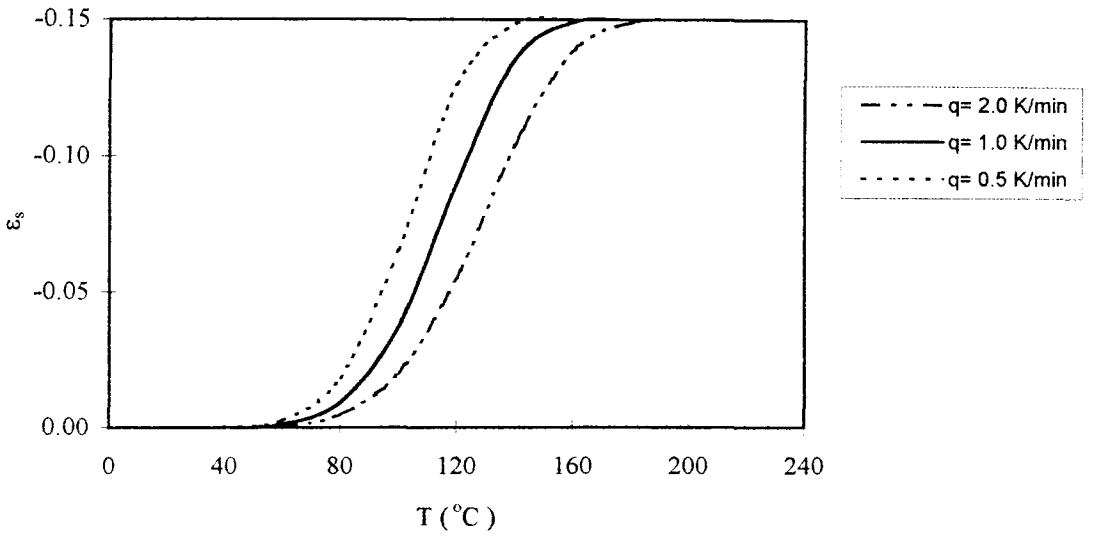

Figure 4.15. Change in syneresis strain with temperature at different heating rates at a thickness of 18cm (G=5 MPa).

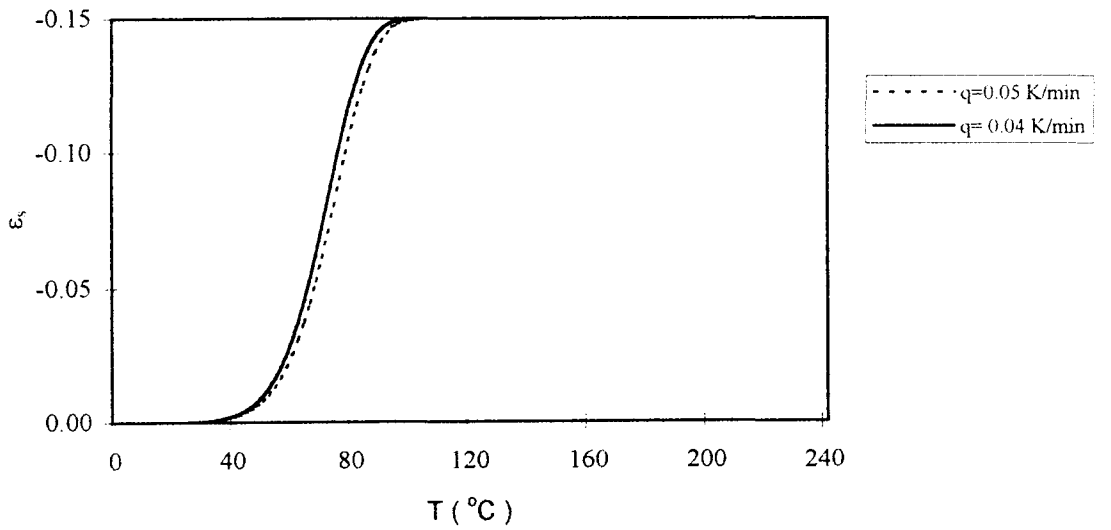

Figure 4.16. Change in syneresis strain with temperature at different heating rates at a thickness of 18cm (G=5 MPa).

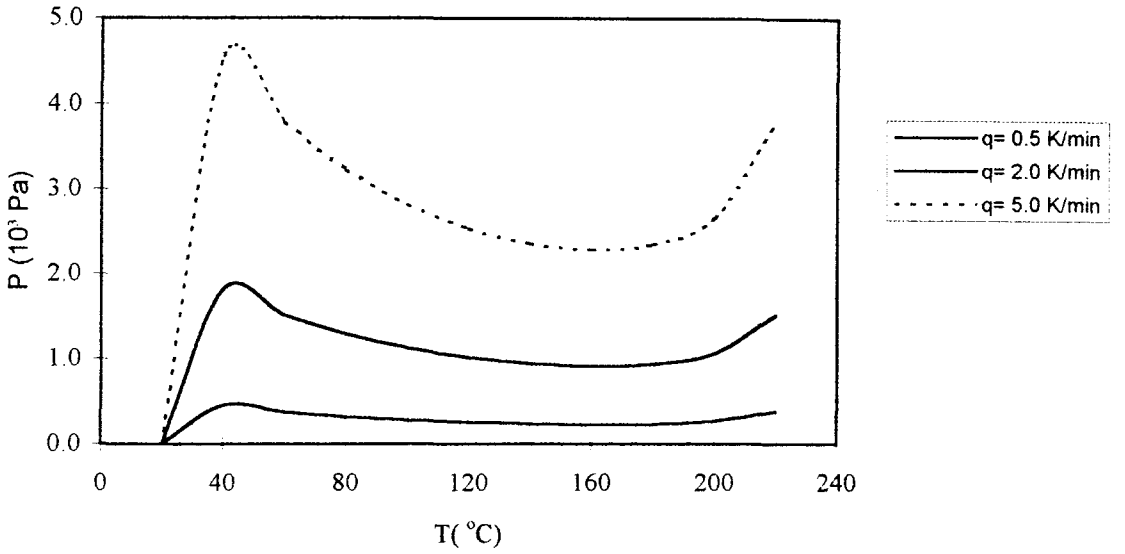

Figure 4.17. Change in stress in the pore liquid with temperature for a plate thickness of 1.0 mm (G=5 MPa).

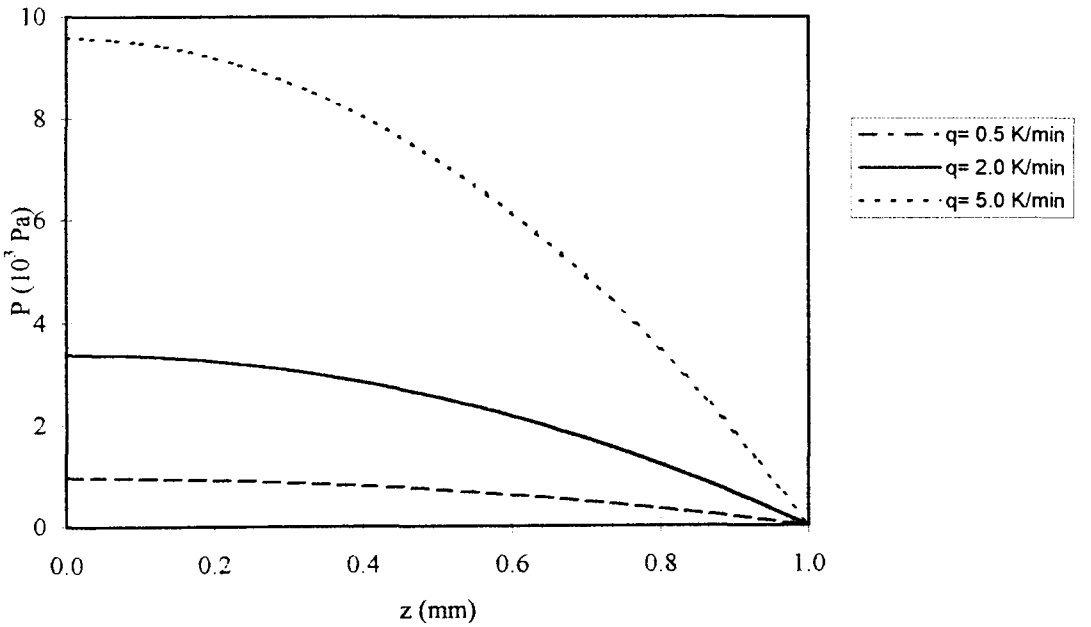

Figure 4.18. Change in stress in the pore liquid with thickness at different heating rates for a temperature of 235 °C (G=5 MPa).

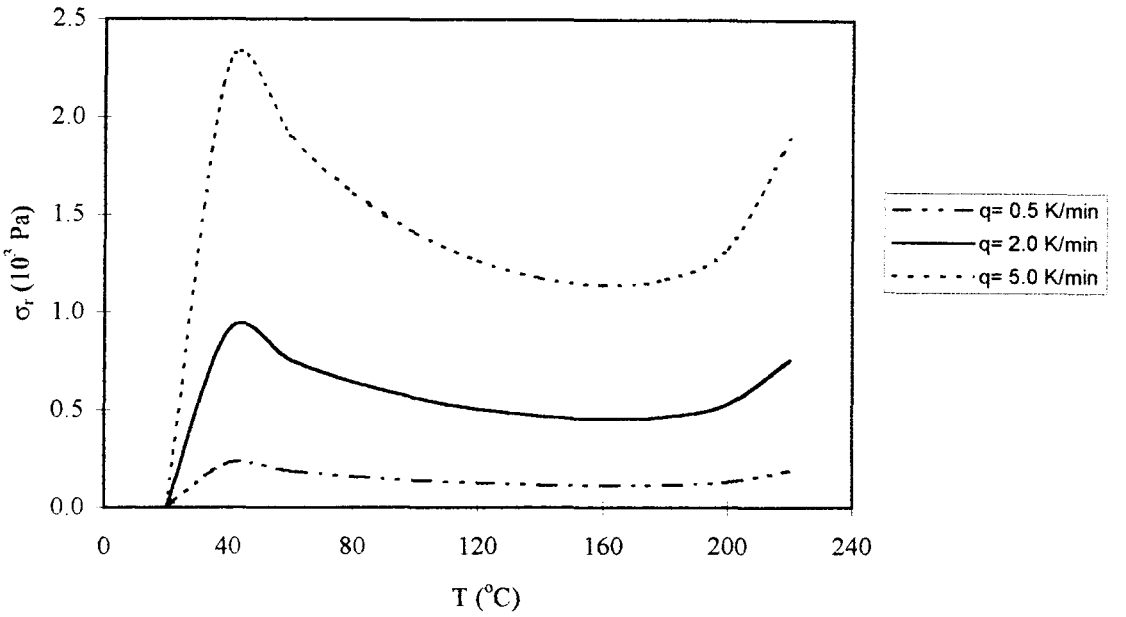

Figure 4.19. Change in radial stress with temperature at different heating rates for plate thickness of 1.0 mm (G=5MPa).

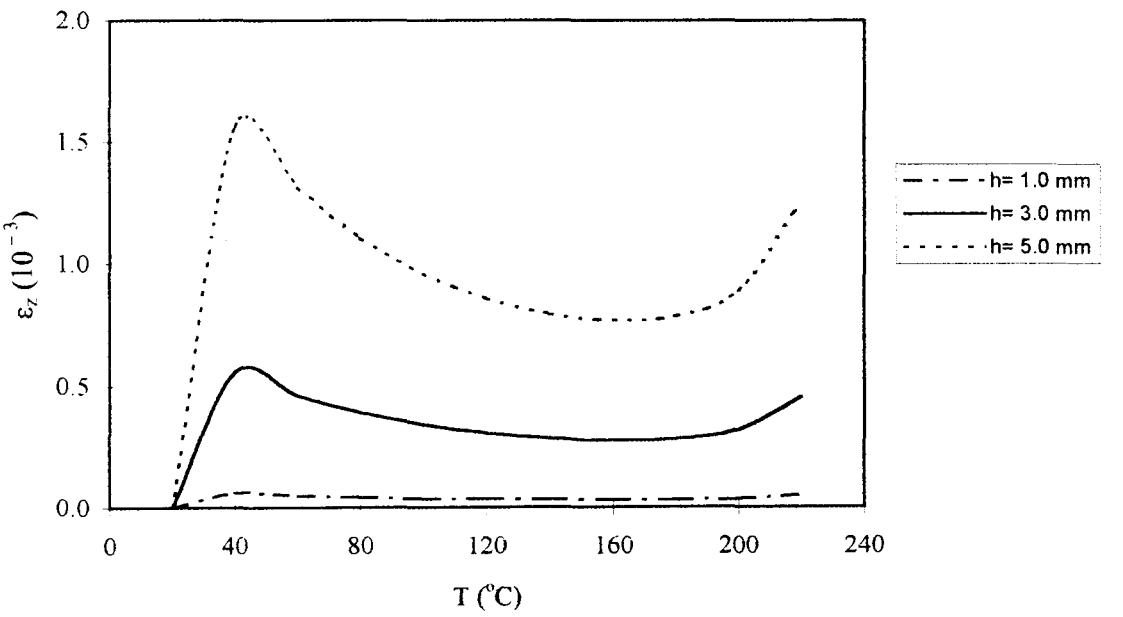

Figure 4.20. Change in strain with temperature for different thicknesses at a heating rate of 2.0 °C/min.

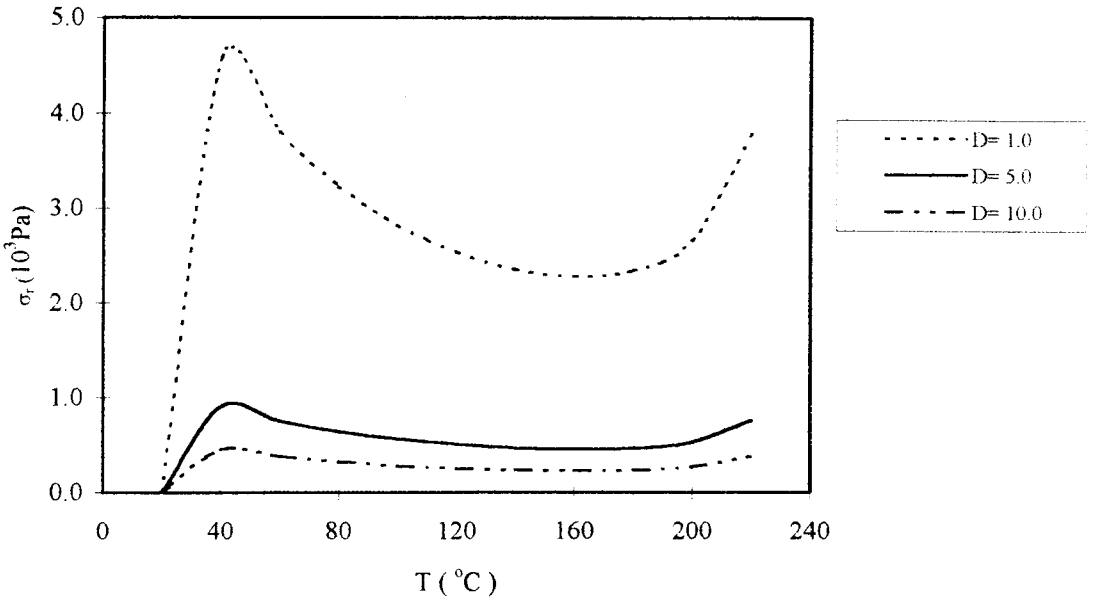

Figure 4.21. Change in radial stress with temperature at heating rate of 2 °C/min and plate thickness of 1.0 mm for different permeabilities (G=5 MPa).

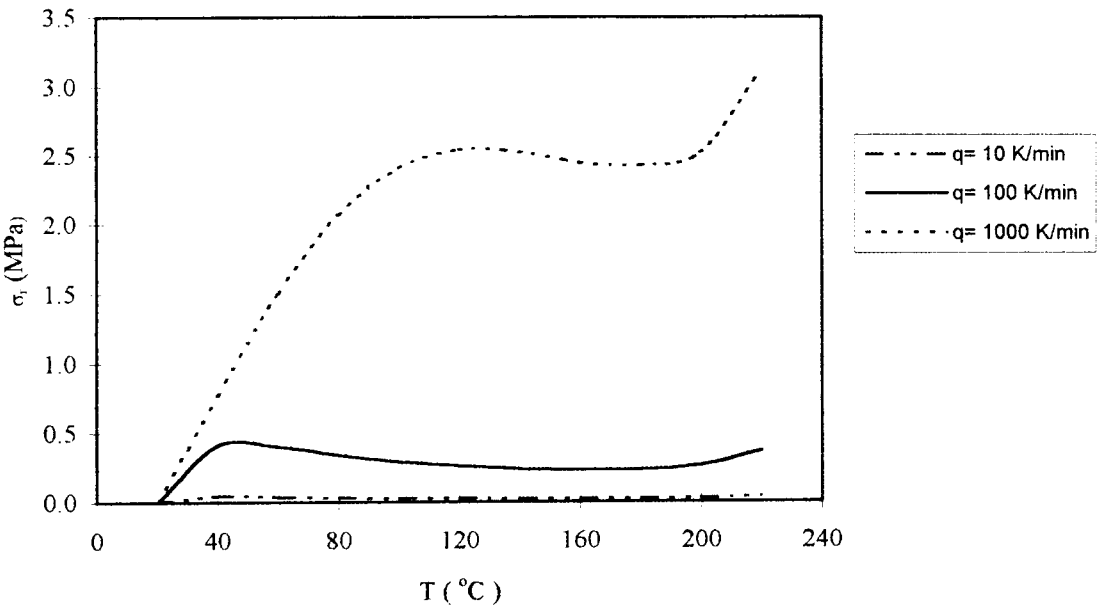

Figure 4.22. Change in radial stress with temperature at different heating rates and plate thickness of 1.0 mm (G=5 MPa).

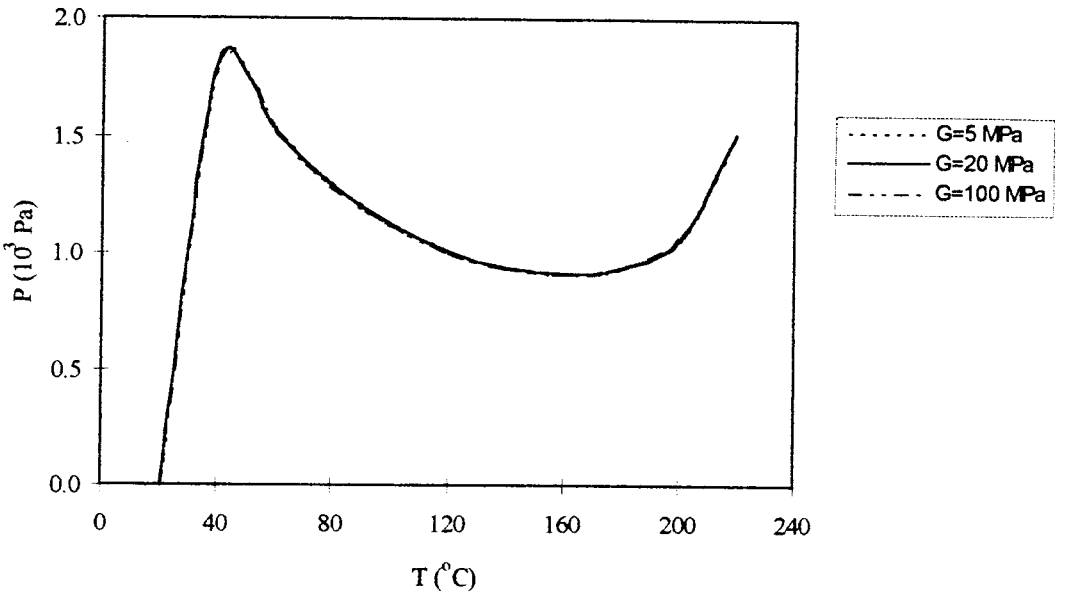

Figure 4.23. Change in stress in pore liquid with temperature at different shear moduli for a heating rate of 2 °C/min and at a thickness of 1 mm.

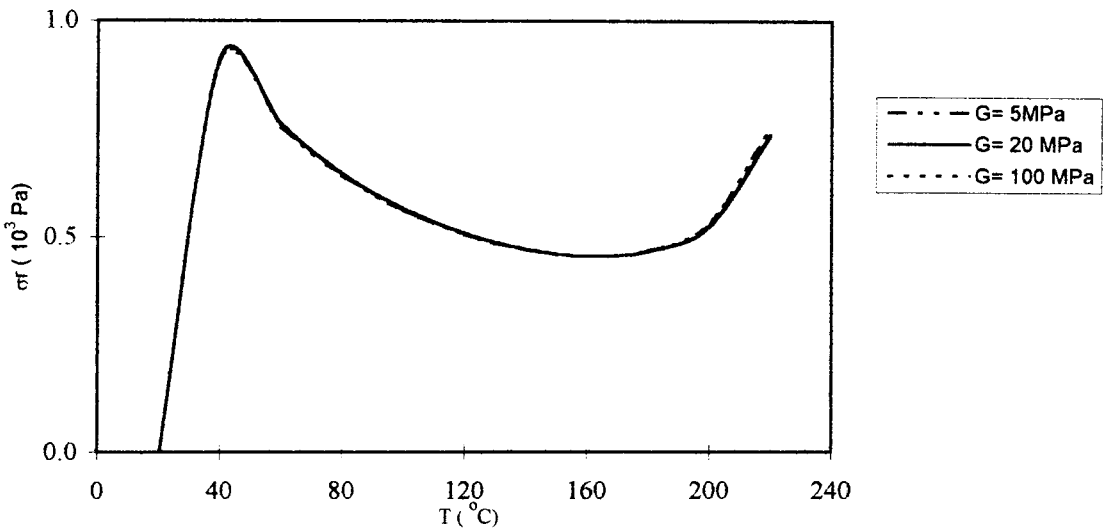

Figure 4.24. Change in radial stress with temperature at different shear moduli for heating rate of 2 °C/min at a thickness of 1 mm.

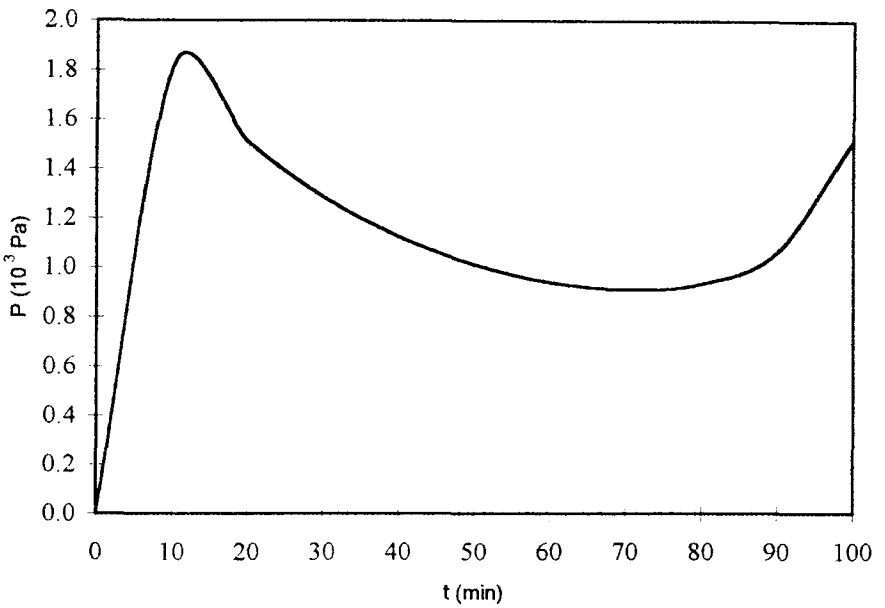

Figure 4.25. Change in stress in pore liquid with time for thickness of 1 mm at a heating rate of 2 °C/min (PDECOL).

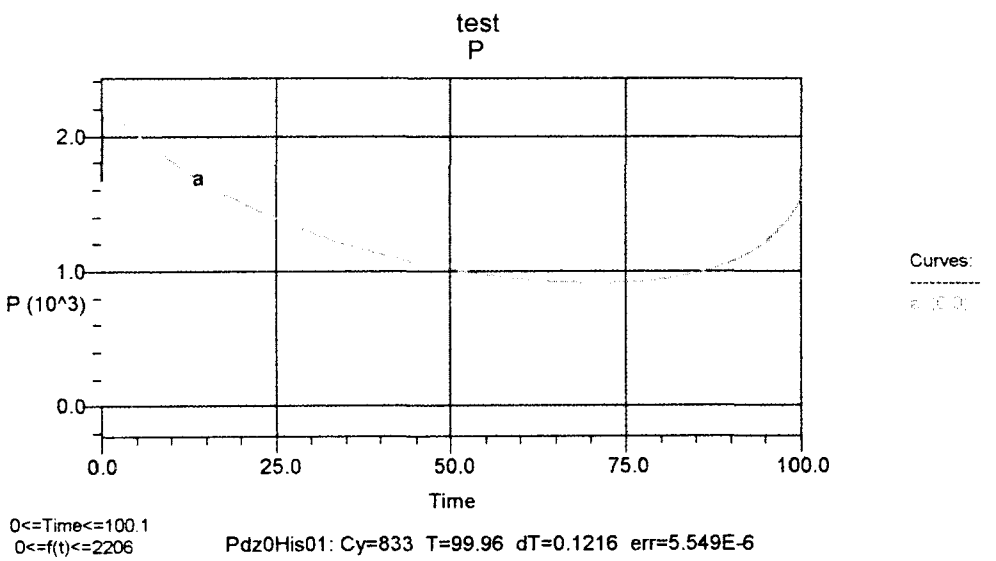

Figure 4.26. Change in stress in pore liquid with time for a thickness of 1.0 mm at a heating rate of 2 °C/min (PDEase2D).

5. CONCLUSIONS AND RECOMMENDATIONS

The following conclusions stated below are drawn from the modeling of stress development in cylindrical silica gel, and a circular plate with radial constraint. Also, recommendations for the future studies are given in the second section of the chapter.

5.1. Conclusions

The modeling of supercritical drying process for the cylindrical geometry results in a partial differential equation with physical boundary constraints in the radial direction. This model is solved using Method of Lines and Finite Element Collocation Procedure via PDECOL and using Galerkin Finite Element Method via PDEase. The solution of model allows following general observations:

For the thin circular plate, stress development is about three orders of magnitude less than the stresses formed in the cylindrical silica gel.

The increase in liquid flux with increasing temperature affects the stress formation significantly in case of the circular plate. It decreases the rate of increase of stress developed and the curves have maxima. On the other hand, this effect is not observed for the cylindrical gel. Instead, the curves increase steadily.

Stress development in the cylindrical silica gel increases an order of magnitude when radial constraint is applied. For the cylinder with radial constraint, increasing heating rate does not bring much difference to the magnitude of the stresses formed, which in contrast to the significant change in stresses with the change in heating rate both for the circular plate and for the cylinder with no constraint. In case of the circular plate, , which is chosen to examine the effect of flash heating, stresses formed exceed the modulus of rupture of the cylindrical gel for flash heating (a heating rate of 1000 °C/min).

Syneresis effect is included only for the cylindrical gel. Magnitudes of stresses increase considerably when syneresis is allowed for. The gel cracks even at a heating rate of 0.04 °C/min which is too slow to have a physical meaning.

Stress formation in cylindrical gel is affected by the change of shear modulus of the network significantly. At higher shear moduli, stress formation is considerably higher. On the other hand, for the circular plate, increase in the shear moduli does not shift the curve.

Increase in the permeability results in significant decrease of stress development in the circular plate.

5.2. Recommendations

In this study, also a model is derived for a circular plate without physical constraint. The model should be solved to compare the cases with and without constraint and to see the effect of radial constraint to stress formation in the alcogel during heating. The model can be applied to different materials after the properties of the gel network are measured. The change in shear modulus, permeability during the process can be included in the study, if a functional form can be developed for these parameters. Also, different steps in supercritical drying process such as heating, diffusion, depressurization can be modeled and these steps can be combined in order to decide on optimum operating conditions.

APPENDIX A

PDECOL

```
C MAIN PROGRAM AND THE USER WRITTEN SUBROUTINES


      PROGRAM ILK
      IMPLICIT REAL*8 (A-H,O-Z)
      COMMON/ENDPT/XLEFT
      COMMON/GEAR0/DTUSED,NQ,NSTEPS,NF,NJ
      COMMON/SOLARIS/H
      REAL HT, KP

      DIMENSION U(1,31),XBKPT(31),SCTCH(10),WORK(5000),IWORK(500)
      DIMENSION EF(1,31), ST(1,31)
      NO=6
      MO=7
      JO=8
      IO=9
      OPEN(NO,FILE='u2d12.ex')
      OPEN(MO,FILE='u2m12.ex')
      OPEN(JO,FILE='u2f12.ex')
      OPEN(IO,FILE='u2s12.ex')
      H=1.0*(10.0**(-3.0))
      KP=133.33*(10.0**6.0)
      HT=2.E-2
      NPDE = 1
      NINT = 30
      KORD = 6
      NCC  =3
      T0   = 0.0
C     TOUT = 1.E-3
      TOUT=0.5
C     DT   = 1.E-4
      DT   = 1.E-9
      EPS  = 1.E-7
      MF   = 21
      INDEX= 1
C
      DO 1 I=1,IWORK(1)
      WORK(I) = 0.0
    1 CONTINUE
      IWORK(1) = 5000
      IWORK(2) =  500
C
      NPTS = NINT + 1
      DX = 1.0/FLOAT(NPTS-1)
      DO 10 I=1,NPTS
      XBKPT(I) = FLOAT(I-1)*DX
   10 CONTINUE
      XLEFT = XBKPT(1)
C
C CALL THE PACKAGE TO INTEGRATE TO TIME  T = TOUT
```

```
C
  20 CALL PDECOL (T0,TOUT,DT,XBKPT,EPS,NINT,KORD,NCC,NPDE,MF,INDEX,
   &           WORK,IWORK)
C
C CHECK FOR EXECUTION ERRORS
C
    IF(INDEX.NE.0) GO TO 70
C
C OUTPUT PERFORMANCE DATA AND COMPUTED SOLUTION VALUES
C
    WRITE(NO,30) TOUT,DTUSED,NSTEPS
  30 FORMAT(//,10X,3HT= ,E10.3,7H   DT= ,E10.3,15H   TOTAL STEPS=,I5)
C
    CALL VALUES (XBKPT,U,SCTCH,NPDE,NPTS,NPTS,0,WORK)
C
    DO 60 K=1,NPDE
    WRITE(NO,40) K
  40 FORMAT(/,10X,13HPDE COMPONENT,I2,/)
    WRITE(NO,50) (U(K,I),I=1,NPTS)
    DO 41 J=1,NPTS
    EF(1,J)=(-2.0*U(1,J))/(9.0*KP)
  41 CONTINUE
    DO 42 J=1,NPTS
    ST(1,J)=(-EF(1,J))*240.0*(10.0**6.0)/0.8
  42 CONTINUE
    WRITE(MO,50) (EF(1,I),I=1,NPTS)
    WRITE(JO,50) (ST(1,I),I=1,NPTS)
      SUM=0.0
     DO 13 I=1,31

    M=1
    IF ((I.EQ.2).OR.(I.EQ.4).OR.(I.EQ.6).
   & OR.(I.EQ.8).
   & OR.(I.EQ.10).OR.(I.EQ.12).OR.(I.EQ.14).
   & OR.(I.EQ.16).OR.(I.EQ.18).OR. (I.EQ.20).
   & OR.(I.EQ.22).OR.(I.EQ.24).OR. (I.EQ.26).
   & OR.(I.EQ.28)) M=4
    IF ((I.EQ.3).OR.(I.EQ.5).
   & OR.(I.EQ.7)
   & .OR.(I.EQ.9).OR.(I.EQ.11).OR.(I.EQ.13).
   & OR.(I.EQ.15).OR.(I.EQ.17).OR.(I.EQ.19).
   &OR.(I.EQ.21).OR.(I.EQ.23).OR. (I.EQ.25).
   &OR.(I.EQ.27).OR.(I.EQ.29)) M=2

    SUM=SUM+M*EF(1,I)*1.5
C     WRITE(*,*)T, SUM
  13 CONTINUE
    SUM1=SUM/90.0

    WRITE(IO,*)SUM1,TOUT
    H=0.001+SUM1*0.001
    WRITE(*,*)'H', H
    COUNTER=COUNTER+1

C     WRITE(*,*) (U(K,I),I=1,NPTS)
  50 FORMAT(10X,5E12.6)
  60 CONTINUE
```

```
C
C SET NEW OUTPUT TIME AND CONTINUE THE INTEGRATION IF TOUT.LT.11.0
C OTHERWISE, TERMINATE THE PROBLEM
C
      TOUT = TOUT+0.5

      IF(TOUT.LT.110.0) GO TO 20
   70 WRITE(NO,80) INDEX
   80 FORMAT(10X,7HINDEX= ,I3)
      CLOSE(NO)
      STOP
      END
C
C .....
      SUBROUTINE F (T,X,U,UX,UXX,FVAL,NPDE)
      IMPLICIT REAL*8 (A-H,O-Z)
      DIMENSION U(NPDE),UX(NPDE),UXX(NPDE),FVAL(NPDE)
      COMMON/SOLARIS/H

      FVAL(1) = (((5.5/1.0*60.0*20.0*(6.0*(1/(H**2.0))))*(10.0**(-12.0))
     &         /((51.9/(293.0+2.0*T))**4.29)) *UXX(1))
     &          -(0.937*1.0/1.0*20.0*(10.0**6.0))*
     &     ((220.0-2.0*T)**(-0.768))
C     FVAL(1) = U(2)*U(2)*UXX(1)-U(1)*U(2)-U(1)**2+10.0
C    &         +2.0*U(2)*UX(2)*UX(1)
      RETURN
      END
C
C .....
      SUBROUTINE BNDRY (T,X,U,UX,DBDU,DBDUX,DZDT,NPDE)
      IMPLICIT REAL*8 (A-H,O-Z)
      DIMENSION U(NPDE),UX(NPDE),DZDT(NPDE)
      DIMENSION DBDU(NPDE,NPDE),DBDUX(NPDE,NPDE)
      COMMON/ENDPT/XLEFT
C
      IF(X.NE.XLEFT) GO TO 10
      DBDU(1,1) = 0.
C     DBDU(1,2) = 0.0
C     DBDU(2,1) = 0.0
C     DBDU(2,2) = 1.0
      DBDUX(1,1) = 1.
C     DBDUX(1,2) = 0.0
C     DBDUX(2,1) = 0.0
C     DBDUX(2,2) = 0.0
      DZDT(1) = 0.0
C     DZDT(2) = 0.0
      RETURN
C   10 DBDU(1,1) = U(2)*COS(U(1)*U(2))
   10 DBDU(1,1) = 1.0
C     DBDU(1,2) = U(1)*COS(U(1)*U(2))
C     DBDU(2,1) = U(2)*SIN(U(1)*U(2))
C     DBDU(2,2) = U(1)*SIN(U(1)*U(2))
      DBDUX(1,1) =0.0
C     DBDUX(1,2) = 0.0
C     DBDUX(2,1) = 0.0
C     DBDUX(2,2) = 1.0
      DZDT(1) = 0.0
C     DZDT(2) = 0.0
```

```
      RETURN
      END
C
C .....
      SUBROUTINE UINIT (X,U,NPDE)
      IMPLICIT REAL*8 (A-H,O-Z)
      DIMENSION U(NPDE)
C
C SET INITIAL CONDITIONS. NOTE THAT PI= 4.0*ATAN(1.0)
C
      U(1) = 0.
C     U(1) = 0.5*(X+1.0)
C     U(2) = 4.0*ATAN(1.0)
      RETURN
      END
C
C .....
      SUBROUTINE DERIVF (T,X,U,UX,UXX,DFDU,DFDUX,DFDUXX,NPDE)
      IMPLICIT REAL*8 (A-H,O-Z)
      DIMENSION U(NPDE),UX(NPDE),UXX(NPDE)
      DIMENSION DFDU(NPDE,NPDE),DFDUX(NPDE,NPDE),DFDUXX(NPDE,NPDE)
      COMMON/SOLARIS/H
C
      DFDU(1,1) = 0.
C     DFDU(1,1) = -U(2)-2.0*U(1)
C     DFDU(1,2) = 2.0*U(2)*UXX(1)-U(1)+2.0*UX(2)*UX(1)
C     DFDU(2,1) = 2.0*U(1)*UXX(2)+U(2)+2.0*UX(1)*UX(2)
C     DFDU(2,2) = U(1)-2.0*U(2)
C
      DFDUX(1,1) =0.
C     DFDUX(1,1) = 2.0*U(2)*UX(2)
C     DFDUX(1,2) = 2.0*U(2)*UX(1)
C     DFDUX(2,1) = 2.0*U(1)*UX(2)
C     DFDUX(2,2) = 2.0*U(1)*UX(1)
C
      DFDUXX(1,1) =((5.5/1.0*60.0*20.0*((6.0*(1/(H**2.0)))))*
     &       (10.0**(-12.0)) /((51.9/(293.0+2.0*T))**4.29))
C     WRITE(*,*) DFDUXX(1,1)
C      DFDUXX(1,1) = U(2)*U(2)
C     DFDUXX(1,2) = 0.0
C     DFDUXX(2,1) = 1.0
C     DFDUXX(2,2) = U(1)*U(1)
      RETURN
      END
```

APPENDIX B

PDEASE2D

{program made using PDEase for h=1.0 mm, q= 2 C/min, G= 5 MPa }

Title

"test"

Select

alias(x)="Radius" alias(y)="Z"

Variables

u

Definitions

g=(1980e-6)

n=(51.9/(293+2.0*t))**(4.29)

expa=0.937e6*(220-2*t)**(-0.768)

r1=1.0

h=1.0

P= -u

Initial Values

u=0

Equations

(g/n)*DYY(u)-expa=dt(u)

Boundaries

region 1

start(0,0)

natural(u)=0 line to (r1,0)

natural(u)=0 line to (r1,h)

value(u) =0 line to (0,h)

Time

0 to 100 by 1

Histories

history(P) at (0.0,0.0)

End

Notifications
Info: Loading PDEase2D Pro v3.0.1 Small Node Limit Engine (32 Equation)
Info: Starting run...
Info: Last Status: Cycle=833 | Time=99.96 | dT=0.1216 | Nodes=149 | Cells=62 | PDE Err=5.549E-6
Info: Run completed.
Normal Exit: PDEase server being shutdown.

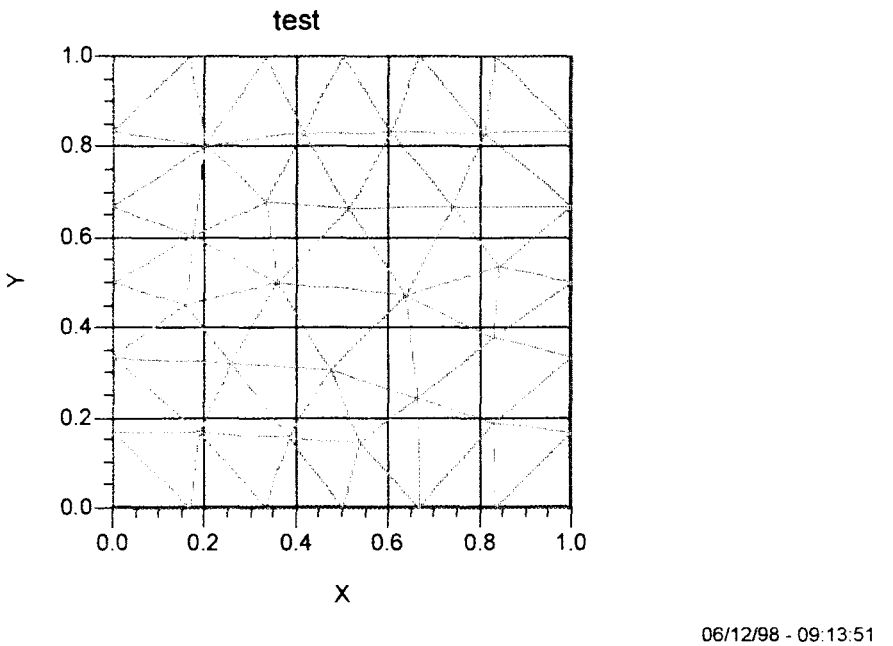

Figure B1. Default Grid Monitor

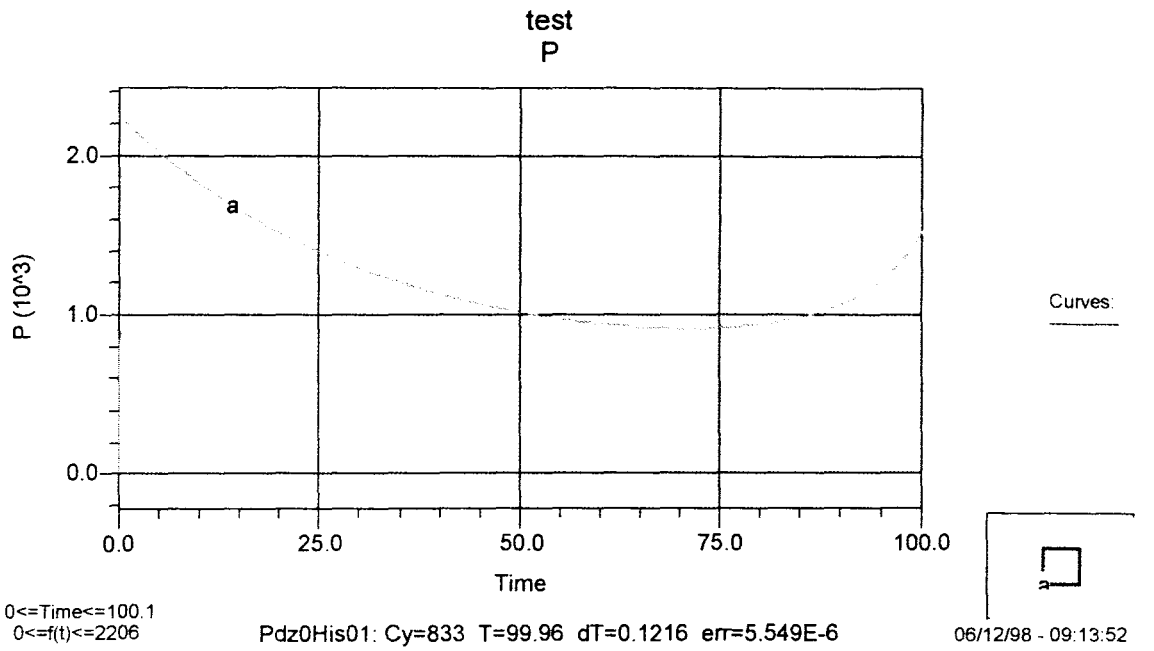

Figure B2. Change in stress in pore liquid with time at a thickness of 1mm and heating rate of 2 °C/min (PDEase2D).

REFERENCES

Ayen, R. J., and P. A. Iacobucci , "Metal Oxide Aerogel Preparation by Supercritical Extraction," *Reviews in Chemical Engineering*, Vol. 5, pp. 157-198, 1988.

Boley, A. B., and Jerome H. Weiner, *Theory of Thermal Stresses*, John Wiley, New York, 1960.

Brinker, C. J., and G. W. Scherer, *Sol-Gel Science*, Academic Press Inc., San Diego, 1990.

Gesser, H. D., and P. C. Goswami , "Aerogels and Related Porous Materials," *Chemical Reviews*, Vol. 89, pp. 765-788, 1989.

Madsen, N. K., and R. F Sincovec,. " Algorithm 540, PDECOL, General Collocation Software for Partial Differential Equations,", *Transaction on Mathematical Software*, Vol. 5 , pp. 326-351, 1979.

McCrum, N. G., C. P. Buckley, C. B. Bucknall, *Principles of Polymer Engineering*, Oxford University Press, Oxford, 1994.

Mulder, C. A. M., and J. G. Van Lierop, "Preparation of Dried Monolithic SiO_2 Gel Bodies by an Autoclave Process," *Journal of Non-Crystalline Solids*, Vol. 82, pp. 265-270, 1986.

Novak Z., and Z. Knez, "Diffusion of Methanol-Liquid CO_2 and Methanol-Supercritical CO_2 in Silica Aerogels," *Journal of Non-Crystalline Solids*, Vol. 221, pp. 163-169, 1997.

Nowinsky, J. L., *Theory of Thermoelasticity with Applications*, Sijthoff & Noordhoff, The Netherlands, 1978.

Pajonk, G. M., "Aerogel Catalysts," *Applied Catalysis*, Vol. 72, pp. 217-23, 1991.

Rangarajan, B., and C. R. Lira, "Production of Aerogels," *The Journal of Supercritical Fluids*, Vol. 4, pp. 1-6, 1991.

Scherer, G. W., "Thermal Expansion of Gels: A Novel Method for Measuring Permeability," *Journal of Non-Crystalline Solids*, Vol. 130, pp.157-170, 1991.

Scherer, G. W., "Stress Development During Supercritical Drying," *Journal of Non-Crystalline Solids*, Vol. 145, pp.33-40, 1992.

Scherer, G. W., "Freezing Gels," *Journal of Non-Crystalline Solids*, Vol. 155, pp.1-25, 1993.

Scherer, G. W., "Stress in Aerogel during Depressurization of Autoclave: 1. Theory," *Journal of Sol- Gel Science and Technology*, Vol. 3, pp. 127-139, 1994a.

Scherer, G. W., "Stress in Aerogel During Depressurization of Autoclave: 2. Silica Gel," *Journal of Sol- Gel Science and Technology*, Vol. 3, pp. 141-150, 1994b.

Schmitt, W. J., R. A. Grieger-Block, T. W. Chapman, "The Preparation of Acid-Catalyzed Silica Aerogel," in M. E. Paulitis and et al. (Eds), *Chemical Engineering at Supercritical Fluid Conditions*, Michigan: An Arbor Science Publishers, pp. 445-460, 1993.

Sunol, S. G., O. Keskin, O. Guney, A. K. Sunol, "Supercritical Fluid Aided Preparation of Aerogels and Their Characterization," *Proceedings of the Third International Symposium on Supercritical Fluids, Tome 3 Reactions, Material Science, Chromatography and Analytical SFE, I.N.P.L. A.R.*, pp. 387-392, Nancy, France, 1994.

Sunol, S. G., A. K. Sunol, O. Keskin, O. Guney, "Supercritical fluid aided preparation of aerogels and their characterization," *Innovations in Supercritical Fluids Science and Technology*, Chapter 17, edited by K. W. Hutchenson and N. R. Foster, ACS Symposium Series, pp. 258-268, 1995.

Sunol, S. G., Z. Tosyali, A. K. Sunol, "Supercritical carbon dioxide aided catalyst design, its characterization and behavior in reacting environment," *in Process Technology Proceedings*, 12: High Pressure Chemical Engineering, Ph. Rudolf von Rohr and Ch. Trepp Eds., pp. 109-114, Lousanne, Elsevier, 1996.

Timoshenko, S. P., J. N. Goodier, *Theory of Elasticity*, McGraw-Hill, New York, 1970.

Ward, D. A., and E. I., Ko, "Preparing Catalytic Materials by the Sol-Gel Method," *Industrial and Engineering Chemistry Research*, Vol. 34, pp. 421-433, 1995.